Potential impacts of electric vehicles on air quality and health endpoints in the Greater Houston Area in 2040

Center for Transportation, Environment, and Community Health
Final Report

by
Shuai Pan, H. Oliver Gao

December 30, 2019

DISCLAIMER

TECHNICAL REPORT STANDARD TITLE PAGE

1. Report No.	2.Government Accession No.	3. Recipient's Catalog No.
4. Title and Subtitle Potential impacts of electric vehicles on air quality and health endpoints in the Greater Houston Area in 2040		5. Report Date December 30, 2019 6. Performing Organization Code
7. Author(s) Shuai Pan, H. Oliver Gao		8. Performing Organization Report No.
9. Performing Organization Name and Address School of Civil and Environmental Engineering Cornell University Ithaca, NY 14853		10. Work Unit No. 11. Contract or Grant No. 69A3551747119
12. Sponsoring Agency Name and Address U.S. Department of Transportation 1200 New Jersey Avenue, SE Washington, DC 20590		13. Type of Report and Period Covered Final Report 03/01/2019 – 02/28/2020 14. Sponsoring Agency Code US-DOT

15. Supplementary Notes

16. Abstract

Significant emissions from transportation contribute to the formation of O_3 and fine particulate matter ($PM_{2.5}$), causing poor air quality and health. In this study, four scenarios were developed to understand how future fleet electrification and turnover of both gasoline and diesel vehicles affect air quality and health in the Houston Metropolitan area. These scenarios considered increased vehicle activity and various configurations of emissions controls. Comparing to a base year of 2013, model predictions for 2040 indicated a ~50% emissions increase in the Business As Usual (BAU) case, and ~50%, ~75%, and ~95% reductions in the three distinct emissions control cases, the Moderate Electrification (ME), Aggressive Electrification (AE), and Complete Turnover (CT) cases, respectively. Each modeling scenario was conducted using a high-resolution (1 km) WRF-SMOKE-CMAQ-BenMAP air quality and health modeling framework, which helped capture urban features in higher detail. The emissions control cases resulted in 1-4 ppb maximum 8h O_3 increase along highways and reductions both in the regions enclosed by the highways and those downwind. Simulated $PM_{2.5}$ concentrations decreased between 0.5-2 $\mu g\ m^{-3}$. Health impact results suggest that increased O_3 and $PM_{2.5}$ concentrations from the BAU case will lead to 122 additional premature deaths with respect to 2013. However, reduced emissions for the control cases (ME, AE, CT) will prevent 114-246 premature deaths. Additionally, about 7,500 asthma exacerbation and 5,500 school loss days will be prevented in the ME case, benefiting younger individuals. The economic benefits generally followed the same trends as health impacts. The analysis framework developed in this study can be applied to other metropolitan areas. The effects of motor vehicle electrification on power plant emissions were estimated using the Argonne National Laboratory's Autonomie data, and indicated the electrification load to be negligible as opposed to projected electricity generation.

17. Key Words	18. Distribution Statement
transportation, electrification, air quality, health impacts, BenMAP	Public Access and a resulting journal publication. Pan et al., 2019. Potential impacts of electric vehicles on air quality and health endpoints in the Greater Houston Area in 2040. Atmospheric Environment, 207, 38-51.

19. Security Classif (of this report)	20. Security Classif. (of this page)	21. No of Pages	22. Price
Unclassified	Unclassified		

Form DOT F 1700.7 (8-69)

Potential impacts of electric vehicles on air quality and health endpoints in the Greater Houston Area in 2040

Abstract

Significant emissions from transportation contribute to the formation of O_3 and fine particulate matter ($PM_{2.5}$), causing poor air quality and health. In this study, four scenarios were developed to understand how future fleet electrification and turnover of both gasoline and diesel vehicles affect air quality and health in the Houston Metropolitan area. These scenarios considered increased vehicle activity and various configurations of emissions controls. Comparing to a base year of 2013, model predictions for 2040 indicated a ~50% emissions increase in the Business As Usual (BAU) case, and ~50%, ~75%, and ~95% reductions in the three distinct emissions control cases, the Moderate Electrification (ME), Aggressive Electrification (AE), and Complete Turnover (CT) cases, respectively. Each modeling scenario was conducted using a high-resolution (1 km) WRF-SMOKE-CMAQ-BenMAP air quality and health modeling framework, which helped capture urban features in higher detail. The emissions control cases resulted in 1-4 ppb maximum 8h O_3 increase along highways and reductions both in the regions enclosed by the highways and those downwind. Simulated $PM_{2.5}$ concentrations decreased between 0.5-2 μg m^{-3}. Health impact results suggest that increased O_3 and $PM_{2.5}$ concentrations from the BAU case will lead to 122 additional premature deaths with respect to 2013. However, reduced emissions for the control cases (ME, AE, CT) will prevent 114-246 premature deaths. Additionally, about 7,500 asthma exacerbation and 5,500 school loss days will be prevented in the ME case, benefiting younger individuals. The economic benefits generally followed the same trends as health impacts. The analysis framework developed in this study can be applied to other metropolitan areas. The effects of motor vehicle electrification on power plant emissions were estimated using the Argonne National Laboratory's Autonomie data, and indicated the electrification load to be negligible as opposed to projected electricity generation.

Keywords: transportation, electrification, air quality, health impacts, BenMAP, WRF-SMOKE-CMAQ

1. Introduction

Estimating transportation emissions trends and associated air quality impacts can provide important insights for requisite control policy. The transportation sector is a major contributor to the concentrations of both nitrogen oxides (NO_x) and volatile organic compounds (VOCs), which react in the presence of sunlight to form ozone (O_3). Vehicular traffic also emits important components of fine particulate matter ($PM_{2.5}$) such as organic and elemental carbon (Roy et al., 2011; U.S. EPA, 2017a). Both O_3 and $PM_{2.5}$ are known to be harmful to human health, causing premature deaths (Bell et al., 2005; Krewski et al., 2009) and severe and minor morbidities (e.g., hospital admissions and asthma exacerbations) (Katsouyanni et al., 2009; Mortimer et al., 2002). The adoption of electric vehicles can lead to significant emissions reductions in the transportation sector (Huo et al., 2012; Nichols et al., 2015). As of 2017, electric vehicles accounted for ~1% of new car sales in the United States (and much

higher in other markets, such as Norway with nearly 30% market share) (Vaughan, 2017). A Bloomberg New Energy Finance report (BNEF, 2016) estimated that 35% of global new car sales would be electric-powered in 2040, that was adjusted to 54% in 2017 considering falling battery costs and possible consumer adoption growth (BNEF, 2017). Policymakers from several countries have announced their commitments of a transition to electric vehicles. For example, Norway has called for all new car sales to be electric by 2025; France, the U.K., and the state of California set goals to achieve the same by 2040; and China aims to electrify 20% of its new cars by 2025 (Walsh, 2017). The implementation of these policies will have large impact on transportation emissions, air quality, and human health.

Several previous studies have assessed the potential impacts of electric vehicles on air quality in various regions. Thompson et al. (2009) found that replacing 20% of the gasoline vehicles with electric vehicles over the northeastern U.S. could reduce MDA8 O_3 by 2-6 ppb, barring a few episodes of significant O_3 increases around Newark and Philadelphia. Brinkman et al. (2010) reported that 100% penetration of electric vehicles in Denver would lower the summertime MDA8 O_3 by 2-3 ppb, excluding a 1-2 ppb increase over the downtown area. Li et al. (2016) reported that fully electrifying all light-duty vehicles would lead to reductions in MDA8 O_3 of 1-2 ppb and mean peak-time O_3 of as much as 7 ppb across Taiwan, except in central metropolitan Taipei (an increase of < 2 ppb). Their findings also indicated that electrification would reduce the annual number of days of O_3 pollution episodes by 40% and $PM_{2.5}$ pollution episodes by 6-10%. Nopmongcol et al. (2017) indicated that 17% of light-duty and 8% of heavy-duty vehicle miles traveled and 17-79% of various off-road equipment types would be targeted for electrification in the U.S. by the year 2030. They reported that electrification would reduce O_3 by less than 1 ppb and $PM_{2.5}$ by 0.5 $\mu g\ m^{-3}$.

To date, no similar quantitative evaluation has been conducted for the Houston Metropolitan Area. This is the 4th largest urban area in the United States and classified as a nonattainment area for ozone (O_3) by the United States Environmental Protection Agency (U.S. EPA) (U.S. EPA Green Book, 2017). It is classified as "Marginal" with a current design value (2015-2017) of 80 ppb. It is also in borderline attainment for fine particulate matter ($PM_{2.5}$). As indicated by the 2013 Houston Galveston Area Council (H-GAC) Regional Goods Movement Plan, the population of the Houston area is projected to grow by 50% in 2040, which will result in increased motor vehicle activity and goods movement in the region if the projections hold true. Their study also projected a doubling of the number of trucks in the region by 2040. Another study by the Texas Transportation Institute projected that the number of trucks in the Houston area would increase by 40%-80% and the number of gasoline vehicles by 30% to 50% by 2040 (TCEQ, 2015). Thus, the Houston Metropolitan Area provides a valuable opportunity to evaluate the impact of increased transportation activity and control strategies (e.g., fleet electrification) on air quality and the subsequent health effects.

In this study, we apply relatively large fleet penetrations of electric vehicles, including a moderate fraction (35%) and an aggressive one (70%), to on-road mobile source sectors in the Greater Houston Area for the year 2040. For assessing the future emissions, another important factor that needs to be considered is fleet turnover, where older motor vehicles are replaced with newer technology, resulting in a significant reduction in emissions (Roy et al., 2014; Liu et al., 2015). Previous studies have

assessed the impact of electrification on transportation emissions (Huo et al., 2012; Nichols et al., 2015) and air quality (Thompson et al., 2011; Soret et al., 2014; Nopmongcol et al., 2017), but few have investigated the corresponding health and economic benefits. Pan et al. (2017b) developed and evaluated a fine-resolution (1×1 km) WRF-SMOKE-CMAQ air quality modeling system to gain an understanding of the concentrations of O_3 and the processes over Houston that drove O_3 formation in September 2013. In this study, we extend this framework by adding a health/benefits model to assess motor vehicle emissions, fleet electrification and turnover, and their associated air quality and health impacts. This study aims to answer the following questions:

(1) How would the mobile activity (e.g., vehicle miles traveled) change in the Houston area by 2040? What are the possible future scenarios corresponding to varying degrees of emission control, fleet electrification and turnover for gasoline and diesel vehicles? Under these scenarios, how would the emissions change in 2040?
(2) What are the magnitudes and spatial distributions of changes in regional O_3 and its precursors as well as $PM_{2.5}$ and its speciated components?
(3) What are the magnitudes of changes in premature mortality, morbidities, and consequent economic benefits? What are the primary factors affecting the health impact results? How do the health results vary by county?

2. Methodology

2.1. Air quality modeling system setup and observational data

This study employed a WRF-SMOKE-CMAQ modeling system that included meteorological, emissions, and chemical transport modeling (a simplified flow chart in Fig. S1). Here, we used the U.S. EPA Community Multi-scale Air Quality (CMAQ) model (Byun and Schere, 2006) version 5.0.2 to model chemical transport, the Carbon Bond 5 (CB05) (Yarwood et al., 2005) and AERO6 mechanisms to simulate gas and aerosol chemistry, respectively, and the Weather Research and Forecasting (WRF) model version 3.7 (Skamarock and Klemp, 2008) to simulate meteorology. This study used the National Centers for Environmental Prediction (NCEP) North American Regional Reanalysis (NARR) data (Mesinger et al., 2004) as input for the WRF model. Emission inputs were prepared using the Sparse Matrix Operator Kernel Emissions (SMOKE) system version 3.6 (Houyoux et al., 2000) using the U.S. EPA 2011 National Emission Inventory (NEI-2011) (U.S. EPA, 2015a; 2015b). Details of WRF physics options and CMAQ configurations are listed in Pan et al. (2017b) and used in previous air quality modeling studies (Li et al., 2016; Pan et al., 2017a).

The 1 km resolution simulation domain covered the eight-county Houston-Galveston-Brazoria (HGB) nonattainment area depicted in Fig. 1. Initial and boundary conditions were obtained from the Air Quality Forecasting system at the University of Houston (AQF-UH) (http://spock.geosc.uh.edu/, Choi et al., 2016) over a larger 12 km grid covering the United States, southern Canada, and northern Mexico (left panel in Fig. 1). Model-measurement evaluation was conducted using the Texas Commission on Environmental Quality (TCEQ) Continuous Ambient Monitoring Stations (CAMS)

network, which provided in-situ ground-level measurements for several chemical species such as NO_x, O_3, and a large suite of VOCs, and the U.S. EPA AirNow network, which provided surface $PM_{2.5}$ measurements.

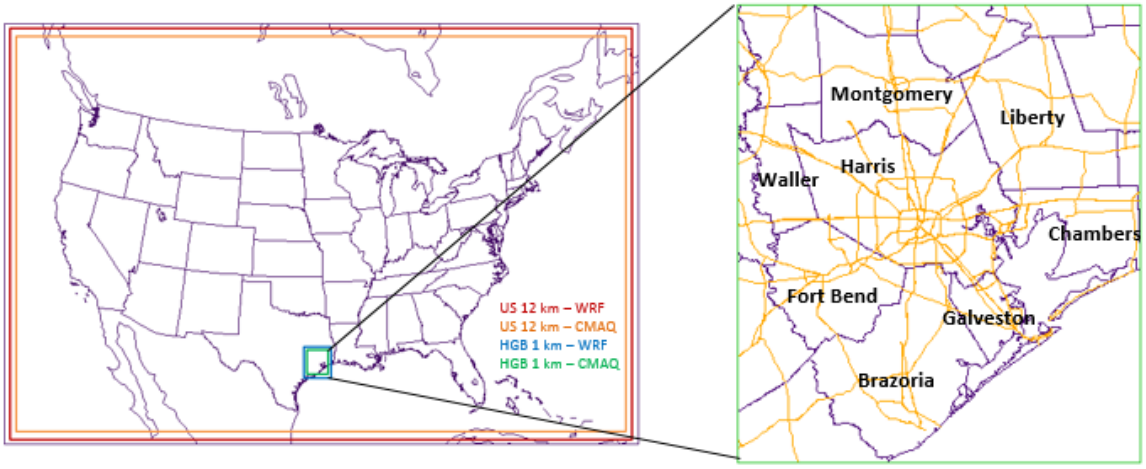

Fig. 1. Horizontal domains of WRF and CMAQ at various grid resolutions; the HGB 1 km is used in this study while the U.S. 12 km is used to provide boundary conditions. In the zoomed-in plot on the right, roadways are represented in orange and county boundaries in purple.

2.2. Mobile source emissions processing

The air quality simulations in this study used emissions from all major sectors, including mobile, point, area, and biogenic sectors. Here, the calculations of on-road mobile emissions were specifically described as we focused on the future change in the transportation sector. This study employed the U.S. EPA Motor Vehicle Emissions Simulator (MOVES) (U.S. EPA, 2016) and SMOKE models to prepare on-road mobile emissions. The MOVES model was ran by U.S. EPA to provide emission factors (EF) look-up tables for mobile emissions as a function of speed, fuel type, vehicle type, road type, and meteorological conditions. The major fuel types include gasoline and diesel, and the vehicle types include motorcycle, passenger car/truck, light commercial truck, intercity/transit/school bus, and medium/heavy duty short-haul/long-haul truck.

In Fig. 2, the "rate-per-distance" (RPD) sector represents on-roadway mobile sources and emission processes. These emissions are located along the roadway networks inside the simulation domain. RPD emissions can be calculated using the following simplified formula:

$$Emission_{RPD} = EF_{RPD} \times hourly\ VMT \quad (1)$$

where the unit of EF_{RPD} is g mile^{-1} and VMT represents vehicle miles traveled.

The "rate-per-vehicle" (RPV) sector represents off-network mobile emissions, which were predominantly concentrated in the urban locations and estimated as follows:

$$Emission_{RPV} = EF_{RPV} \times VPOP \quad (2)$$

where the unit of EF_{RPV} is g vehicle^{-1} hour^{-1}, and $VPOP$ denotes the vehicle population in numbers.

Two other mobile sectors were included: the "rate-per-profile" (RPP), which represents off-network vapor-venting emissions from parked vehicles, was estimated in the same way as RPV; and the "rate-per-hour" (RPH), which includes only extended idle exhaust emissions from on-roadway long-haul trucks, also known as "hoteling". The unit of the emission factor for the RPH is g hour^{-1}, and the RPH's activity data are hoteling hours (Hoteling).

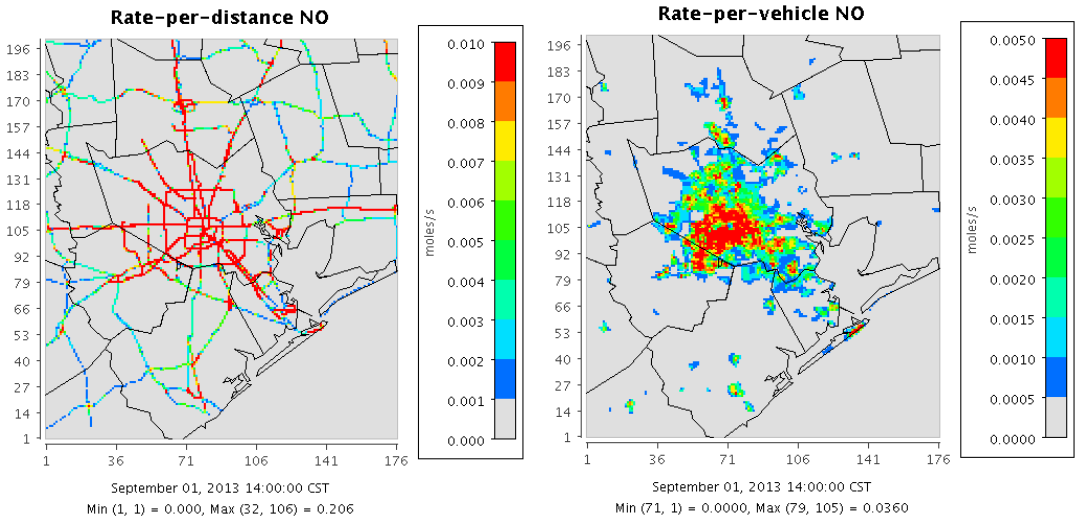

Fig. 2. Spatial distributions of NO emissions from various mobile source sectors at 1400 CST on September 1, 2013. The left panel depicts rate-per-distance and the right panel plots rate-per-vehicle. The sectors include both gasoline and diesel sources.

The activity data (e.g., VMT, VPOP, and Hoteling) came from NEI-2011 and varied by county, month, and source attributes such as fuel type, vehicle type, road type, and emission processes. The activity data were originally submitted by state/local/tribal air agencies to the U.S. EPA. The SMOKE model took EF (the output from MOVES), county-level monthly activity data, and temperature data and produced hourly gridded CMAQ-ready emissions.

2.3. Projections of mobile activity data

Future projections for VMT and VPOP were estimated from calculations performed by the Texas Transportation Institute (TTI) for the Texas Commission on Environmental Quality (TCEQ, 2015). The results are plotted in Fig. 3. Here, panel (a) represents the aggregate VMT (gasoline+diesel) for each of the counties, and panel (b) represents the scaling factors, indicating an increase in VMT from 2013 to 2040 by 30%-80% over the eight-county area. Two surrogate gasoline-diesel split profiles, Houston and Beaumont, were developed for the eight-county area. In panel (c), the gasoline-diesel split for VMT was 93%-7% for Houston and 82%-18% for Beaumont in 2013. The split changes marginally in favor of diesel in 2040, 92%-8% for Houston and 81%-19% for Beaumont. The diesel fractions are higher over suburban Beaumont while gasoline activities are significantly higher in the urban region (i.e., the city of Houston). The Houston profile was used to represent the Brazoria, Fort Bend, Galveston, Harris,

Montgomery, and Waller Counties and the Beaumont profile was used to represent the Chambers and Liberty Counties. The projected gasoline and diesel VMT in 2040 are plotted in panels (d) and (e), with their specific scaling factors in (f). The projected gasoline VMTs are roughly one order of magnitude higher than diesel VMTs because of the greater population of gasoline-powered vehicles. The projected gasoline and diesel scaling factors closely mirror the total VMT, indicating that the change in VMT is more significant than that in the gasoline-diesel split. One subtle difference: the diesel scaling factors are slightly magnified, while the gasoline ones are slightly depressed. For example, in Harris County, the total VMT changes by a factor of 1.46, while the diesel VMT changes by 1.59 and gasoline by 1.45. This slight magnification in diesel scaling factors could be attributed to the marginal shift in favor of diesel (~9% increase) as shown in panel (c). The projected VMT profiles were also used for county and fuel-specific vehicle population (VPOP) and hoteling projections.

Table 1. Descriptions of the simulation scenarios.

Simulation Scenario	% Fleet Turnover New	% Fleet Turnover Electric	% Fleet Turnover Current	Scaling Factor for EFs
Base year (BASE)	0	0	100	1
Business As Usual (BAU)	0	0	100	1
Moderate Electrification (ME)	33	35	32	0.3365
Aggressive Electrification (AE)	15	70	15	0.1575
Complete Turnover (CT)	65	35	0	0.0325

2.4. Design of scenarios

This study designed several emissions scenarios to account for uncertainties in fleet turnover and electrification. In Table 1, "New" indicates the percentage of the fleet in 2040 that uses or is retrofitted with state-of-the-art combustion and emission control technologies. "Electric" represents the percentage of fleet comprising electric vehicles, and "Current" represents the fraction carrying over from the base year of 2013 that is neither retrofitted nor replaced. The "Scaling factor" in the last column is a function of both control technology efficiency and fleet turnover, applied to aggregate (distance, vehicle, profile, and hoteling) gasoline and diesel emissions. The simulation scenarios are as follows:

(1) A "Base year" (BASE) case, representing the month of September 2013, serves as the base case to which future scenarios were compared.
(2) A "Business As Usual" (BAU) case, representing the "worst case" scenario, in which all vehicles in 2040 will have the same emission factors as in 2013.
(3) A "Moderate Electrification" (ME) case, representing a mix where 35% of vehicles will be electric-powered based on the assumptions of a Bloomberg New Energy Finance report (BNEF, 2016), and the remaining fleet will be equally apportioned between vehicles with emissions factors like those in 2013 and new vehicles with improved emission factors.
(4) An "Aggressive Electrification" (AE) case, representing a mix in which 70% of the Houston region fleet is electrified, and the remaining fleet are equally apportioned between vehicles with emissions factors like those in 2013 and new vehicles with improved emissions factors.

(5) A "Complete Turnover" (CT) case, representing the "best case" scenario, in which the total fleet comprise either state-of-the-art combustion technology or electric vehicles.

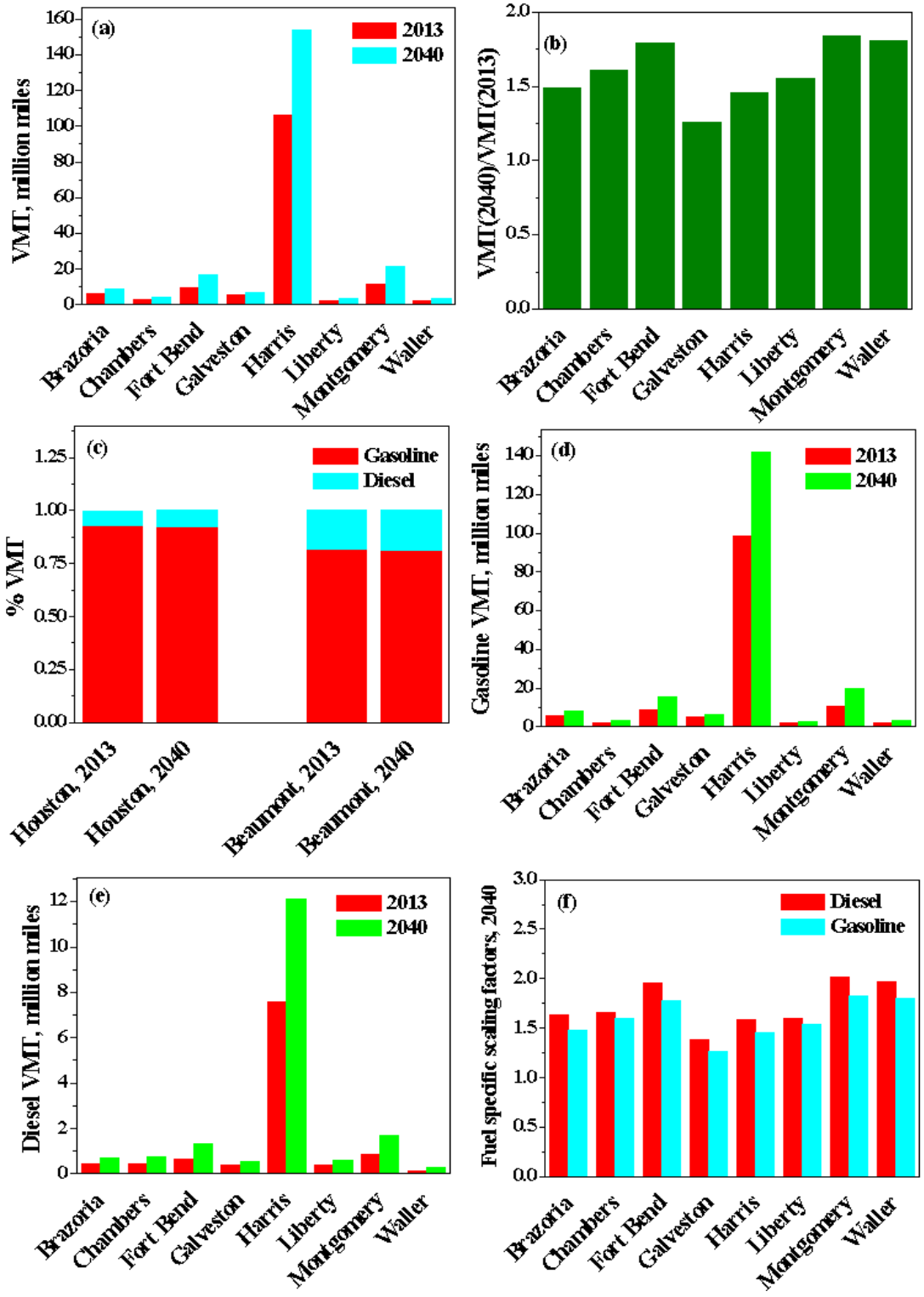

Fig. 3. Future VMT projections for fuel types and counties: (a) the aggregate on-road mobile VMT for each of the counties in 2013 and 2040; (b) the ratio of the aggregated VMT in 2040 to 2013; (c) the

gasoline-diesel split of VMT; (d) similar to panel (a) but for gasoline VMT; (e) similar to panel (a) but for diesel VMT; (f) similar to panel (b) but for gasoline and diesel separately. These projections are based on calculations performed by the Texas Transportation Institute (TTI) for the Texas Commission on Environmental Quality (TCEQ, 2015).

For all future year scenarios, mobile activity data (e.g., VMT, VPOP, and Hoteling) were increased to the 2040 level, and projections of coal and natural gas EGUs were also applied.

2.5. Scaling factors for mobile emission factors

The effective emission factor calculation as described in the U.S. EPA's National Mobile Inventory Model (NMIM) is as follows:

$$EF_i(2040) = EF_i(2013)\left[f_{replaced}(1 - f_{control}) + 1 - f_{replaced}\right] \quad (3)$$

where $EF_i(2040)$ and $EF_i(2013)$ are the emission factors for 2040 and 2013, respectively, $f_{replaced}$ represents the cumulative fraction of the fleet that has been replaced by newer, lower emitting sources between 2013 and 2040, and $f_{control}$ represents the fractional reduction of emissions brought about by this fleet replacement. The value of $f_{control}$ was assumed to be 95% based on Roy et al. (2014). To include the portion of electric vehicles, the original Equation (3) was modified as follows:

$$EF_i(2040) = EF_i(2013)[f_{New}(1 - f_{control}) + f_{Electric} \times 0 + f_{Current}] \quad (4)$$

where f_{New}, $f_{Electric}$, and $f_{Current}$ are the percentage fleet turnover values in Table 1. The scaling factor values listed in Table 1 were obtained using equation (4). For instance, the scaling factor in the ME case was: $0.33 \times (1 - 0.95) + 0.35 \times 0 + 0.32 = 0.3365$. It should be noted here we assumed zero emissions from electric vehicles for easier demonstration. Electric vehicles produce no tailpipe exhaust emissions. However, non-exhaust emissions (e.g., particulate matter emissions from brake and tire wear) would not be significantly reduced and require technology improvement from those emission modes (Soret et al., 2014).

2.6. Electricity demand and projections of EGUs

The added electricity required to power the motor vehicle fleet could potentially result in increased emissions from Electricity Generating Units (EGUs). However, projections by the Electricity Reliability Council of Texas (ERCOT, Borkar, et al., 2016) have indicated that the projected electricity generation will be in western Texas, resulting in no new emissions in the eight-county area. Additionally, ERCOT projections indicate a significant retirement of fossil-fired capacity for southeastern Texas. Despite adding future capacity in the Houston region in our simulations, we needed to account for capacity downsizing in order to represent a more realistic scenario in 2040. Assuming a linear decline trend starting from 2013, we estimated factors of 0.89 and 0.99 (11% and 1% reductions) and applied them to future EGUs powered by coal and natural gas, respectively.

Even though ERCOT projections indicate no new emissions in the Houston area, it is still necessary to calculate the incremental electricity demand due to the vehicle electrification. Here, the

calculation was performed for the Aggressive Electrification scenario, which represented the highest electricity consumption for electric vehicles and hence provided bounding estimates. The VMT data from Fig. 3 were fractionated into New, Electric, and Current types. Each vehicle type was multiplied using its specific energy consumption value per unit mile. Projections for electricity consumption (Wh $mile^{-1}$) for cars were taken from the Argonne National Laboratory (ANL)'s Autonomie model output. For this, the Autonomie data on vehicle types had to be mapped to its MOVES counterpart. For example, the energy consumption for a MOVES passenger car was assumed to be half that of Autonomie compact and midsize combined. The mapping is detailed in Table S1. Electricity data for trucks were adopted from the ANL's AFLEET model (Burnham, 2017). The energy consumption values (in Table S2 and S3) for each vehicle type, per unit mile, were multiplied with their specific VMT values and summed up across all vehicle types to get a total electricity requirement. Additional details for this calculation are listed in Section S2 of the Supplemental Information. The calculations for additional electricity requirement indicated projected electrification load to be negligible (< 1%) of the existing power plant generation. The reasons behind the low fraction could be the fact that Autonomie projections account for improved technology and efficiency in 2040 representing lower energy consumption. This coincides with the BNEF calculations that even as EVs represent 53% of global new car sales, they only take up a small faction (~5%) of global power generation in 2040 (BNEF, 2017). Hence, the incremental electricity demand was not considered in our simulations.

2.7. The health impact model

To evaluate the impact of these various scenarios on health and economic costs in the year 2040, we used the U.S. EPA Environmental Benefits Mapping and Analysis Program (BenMAP) Community Edition version 1.3 (U.S. EPA, 2017b). The air quality inputs of the model include a baseline scenario (without control) and a control scenario (with an emission control policy implemented). In this study, the base year case (2013) is the baseline scenario and the future year cases are different control scenarios. The health impact calculations in BenMAP are based on concentration-response (C-R) functions, typically representing a decrease in adverse health effects with a concentration of air pollutants (Fann et al., 2012). One group of widely used C-R functions are in the log-linear format:

$$\Delta y = \left(1 - e^{-\beta \cdot \Delta x}\right) \times y_0 \times Pop \qquad (5)$$

where Δy represents the change in the incidence of adverse health effects, β the concentration-response coefficient, Δx change in air quality (e.g., O_3 concentrations), y_0 the baseline incidence rates, and Pop the affected population. The relationship between changes in air pollutant concentrations and incidence of health outcome (i.e., β) are usually assessed in epidemiological studies. Additionally, the BenMAP model calculates the economic cost of avoided premature mortality using a "value of statistical life" (VSL) approach, which is the aggregate monetary value that a large group of people would be willing to pay to slightly reduce the risk of premature death in the population (U.S. EPA, 2017b). The economic costs for morbidities were estimated using the cost of illness, which includes direct medical costs and lost earnings associated with illness.

In our analyses, two pollutant metrics were used: maximum daily 8-hr average (MDA8) for O_3 and daily 24-hr mean for $PM_{2.5}$. We used the PopGrid program (U.S. EPA, 2017b) to allocate the 2010 block-level U.S. Census population data to our study domain. The county-level population growth rates for each year from 2000 through 2050 were developed by Woods & Poole (2015) and pre-installed in the BenMAP model. We first evaluated the health endpoint of "Mortality, All Cause". For O_3, we chose C-R coefficient based on the epidemiological studies by Bell et al. (2005), Zanobetti and Schwartz (2008), and Levy et al. (2005), and for $PM_{2.5}$, we chose a study by Krewski et al. (2009). These studies were chosen as their analyses were based on a large geographic area (e.g., 116 U.S. cities in Krewski et al. (2009)). Hence, they are likely to be more representative and applicable to our analysis in the Houston area. Moreover, we also examined several O_3-induced morbidities (e.g., asthma exacerbation, emergency room visits). Because the health impact functions for morbidities were derived from fewer cities or smaller time-scale sample sizes, the functions from several epidemiological studies (listed in Table 2) were used to estimate the risk outcome.

Table 2. The concentration-response functions for the O_3-induced health endpoints used in this study.

Health Endpoint	Start Age	End Age	Risk Estimate, β	Reference
Asthma exacerbation, one or more symptoms	6	18	0.00929 0.00097 0.00222	Mortimer et al., 2002 O'Connor et al., 2008 Schildcrout et al., 2006
Emergency room visits, Asthma	0	99	0.00306 0.00398 0.00521 0.00087 0.00111 0.00300	Glad et al., 2012 Ito et al., 2007 Ito et al., 2007 Peel et al., 2005 Sarnat et al., 2013 Wilson et al., 2005
Emergency room visits, Asthma	0	17	0.01044	Mar and Koenig, 2009
Emergency room visits, Asthma	18	99	0.00770	Mar and Koenig, 2009
School loss days	5	17	0.01576 0.00782	Chen et al., 2000 Gilliland et al., 2001
Hospital admission, All respiratory	65	99	0.00061 0.00064	Katsouyanni et al., 2009

3. Results

3.1. Evaluation of the base year modeling

Domain-wide statistics of model-measurement comparisons for surface O_3 and its precursors between base year model output and in-situ measurements for September 2013 are listed in Table 3. The results are similar to the 4 km simulations of Li et al. (2016) and Pan et al. (2015; 2017a). The time-series comparisons are presented in Fig. S3. For each species, the simulated concentrations generally reproduced the daily variations in the observations during the simulation period.

Table 3. Model evaluation of surface chemical species concentrations for September 2013.

Species	N	IOA	MAE	MB	OM	MM
O_3	26651	0.75	14.3	12.4	24.3	36.7
NO_x	14264	0.71	5.7	0.1	8.6	8.7
CO	6885	0.68	70.7	-42.6	186.9	144.4
Ethylene	4776	0.51	1.7	0.5	1.7	2.2
Toluene	4766	0.55	0.6	0.2	0.6	0.9
Xylenes	4766	0.56	0.3	0.1	0.3	0.4
$PM_{2.5}$	6166	0.45	6.9	1.0	9.9	10.9

Notation: N – Number of data points; IOA – Index of Agreement; MAE – Mean Absolute Error; MB – Mean Bias; OM – Observed Mean; MM – Model Mean. Units of MAE/MB/OM/MM for chemical species: ppb.

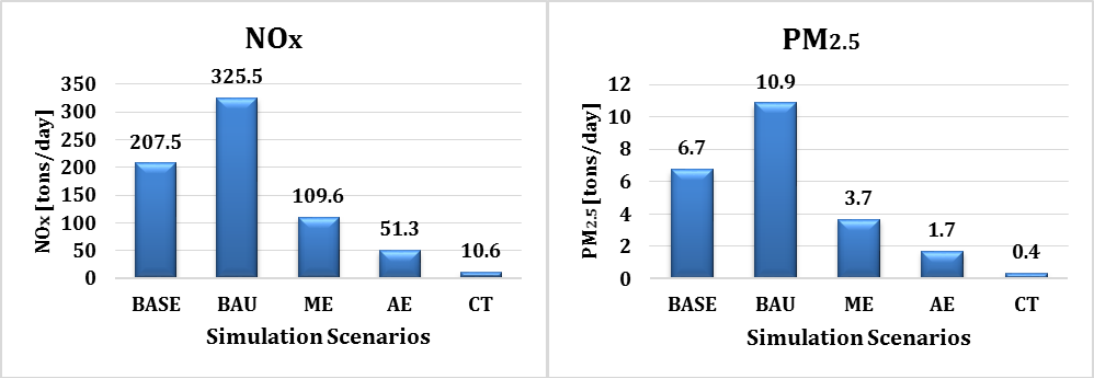

Fig. 4. Episode-average eight-county aggregated on-road mobile emissions [Unit: tons/day] in each simulation scenario for NO_x and $PM_{2.5}$.

3.2. Changes in on-road mobile emissions in the future scenarios

Because the emissions inventory is "ground-zero" for the modeling framework, a comparison of pollutant emissions for each scenario provides insight into the corresponding air quality changes. Fig. 4 plots the episode-average eight-county aggregated on-road mobile emissions in each simulation scenario for NO_x and $PM_{2.5}$. As expected, the Business As Usual case exhibits significant increases in species emissions with respect to the base year, resulting from an increase in vehicles on the road without emissions controls/retrofits. The other cases show various levels of emission reductions. Table S4 lists base year emissions and percentage changes in future year cases for major pollutants. The VOCs include important air toxic species, such as formaldehyde, acetaldehyde, acrolein, and naphthalene, which have high risk factors for cancer. Compared to the BASE case, the fractional changes are ~50% increase in the BAU case, and ~50%, ~75%, and ~95% reductions in the Moderate Electrification, Aggressive Electrification, and Complete Turnover cases, respectively. These changes in emissions are consistent with the assumptions used to develop these scenarios.

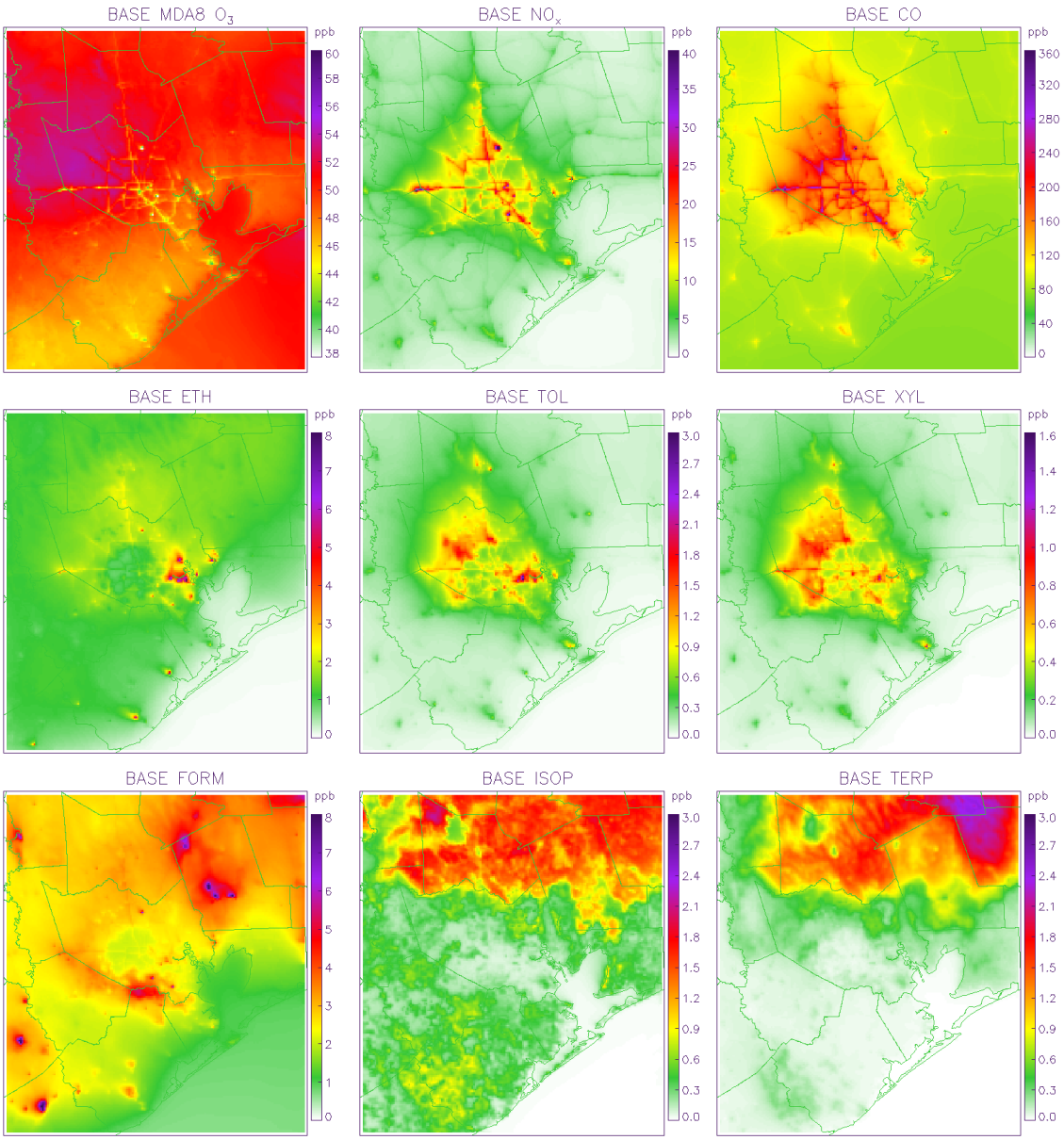

Fig. 5. Spatial distributions of the surface concentrations of monthly average MDA8 O_3, NO_x, CO, ethylene, toluene, xylenes, formaldehyde, isoprene, and terpenes during September 2013 for the BASE case.

3.3. Spatial distributions of pollutants concentrations and projected future changes

3.3.1. Ozone and its precursors

Because O_3 is a secondary pollutant, understanding the distributions of O_3 precursors such as NO_x and dominant highly reactive VOC species is useful. Fig. S4 lists the descriptions of VOC species in the CB05 chemical mechanism and the averaged VOC speciation from on-road mobile emissions in the BASE case. The major highly reactive VOCs are ethylene (ETH, 4.8%), olefin (OLE+IOLE, 3.5%), toluene (TOL, 2.6%), and xylenes (XYL, 2.8%). The paraffin (PAR, or alkanes) are only weakly

reactive with OH and ionic substances, even though they account for ~70% of the total on-road mobile emissions. Fig. 5 plots the spatial distributions of base year surface O_3 and its precursors (e.g., NO_x, CO, and several highly reactive VOC species). The MDA8 O_3 hotspots are located northwest of the urban center, where predominant wind originates from Galveston Bay and the Gulf of Mexico to the southeast (Pan et al., 2017a). High NO_x and CO concentrations are located over the urban area because of high motor vehicle emissions. It is important to identify that NO_x contours are steeper than CO due to the shorter lifetime of NO_x. While elevated ethylene concentrations are predicted over industrial regions, toluene and xylenes concentrations are high over both industrial regions and urban road networks. Formaldehyde hotspots coincide with non-point source oil and gas production regions, and isoprene and terpenes concentrations are high over the northern part of the domain, resulting from significant biogenic emissions generated by large forest cover.

Fig. 6 plots the CMAQ-simulated NO_x and MDA8 O_3 concentrations for each scenario. The results, shown in panels (a)-(d), plot a decrease in absolute NO_x concentrations with increasing fleet turnover, electrification, and control. For example, concentration hotspots are predicted over all highway loops over Houston for the BAU case, and are predicted to significantly decrease in the CT case. In other words, partial fleet electrification accompanied by complete fleet turnover result in lower NO_x emissions and thus, lower concentrations. Panels (i)-(l), which plot O_3 concentrations, tell a different story. The BAU case shows lowered MDA8 O_3 concentrations over the highway loops and higher concentrations elsewhere. Because highways have significant NO_x emissions, they are NO_x-saturated. In such areas, O_3 and NO_x concentrations are inversely correlated, as previous studies (e.g., Choi et al., 2012) illustrated. In addition, panel (i) illustrates increased O_3 concentrations over regions northwest of the loop, resulting from O_3 formation in the outflow of NO_x-saturated areas. The outflow regions are NO_x-limited and provide favorable conditions for O_3 formation. With tighter controls, increased fleet turnover, and decreasing NO_x concentrations, O_3 concentrations increase along the highway loop and decrease over the outflow. Similar findings are corroborated in panels (m)-(p), which show the effects of the O_3 impacts vis-à-vis the 2013 base case. It is predicted that O_3 concentrations resulting from increased motor vehicle emissions decrease in the BAU case over the NO_x-saturated areas by 1-3 ppb while increasing 1-2 ppb over the outflow. Increasing controls, retrofits, electrification, and turnover lead to lower NO_x emissions and an increase in O_3 concentrations by 1-3 ppb over the highways but decrease over the entire outflow surrounding the highway loop, as well as the areas enclosed by the loop. Notably, the CT case exhibit a decrease of 3-4 ppb over the northwestern outflow, the same region where a significant O_3 increase is predicted in the BAU case. Fig. S5 displays the spatial differences for CO, ethylene, and isoprene. The distributions of the change in CO and ethylene concentrations in future year cases are similar to those in NO_x concentrations. Whereas large positive changes in simulated isoprene concentrations exist for the control cases over the northern domain, the decrease in isoprene concentrations in the BAU case could be attributed to more indirect reactions with the enhanced NO_x emissions and concentrations (Diao et al., 2016). In high-NO_x conditions, NO_x serves as a sink for isoprene. Isoprene reaction with hydroxyl radical (OH) in the presence of nitrogen oxide (NO) forms isoprene nitrate or converts NO to NO_2, which can undergo photolysis to form O_3.

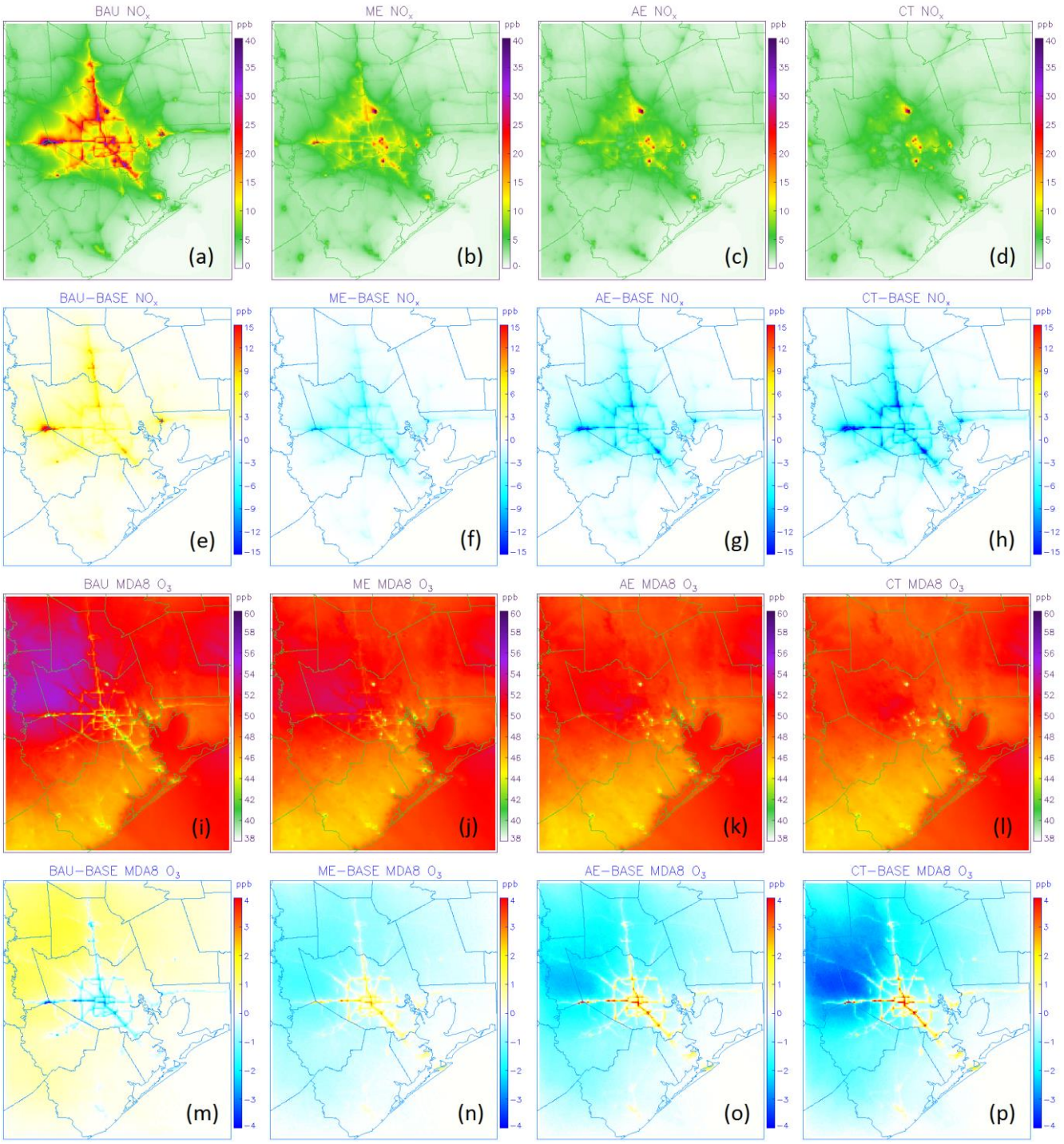

Fig. 6. The spatial distributions of episode-average surface concentrations of NO_x and MDA8 O_3 in each future year scenario (2040) and the spatial differences between the simulations (future year case, 2040 – BASE, 2013). Panels (a)-(d) plot absolute NO_x concentrations, (e)-(h) differences between the future scenarios and base case, (i)-(l) absolute MDA8 O_3, and (m)-(p) differences from the base case.

Fig. S6 plots the differences in MDA8 O_3 between the CT case and BASE case on selected days with relatively large value differences (~10 ppb over downwind regions). Whereas the positive

difference areas are always located over the NO_x-saturated urban roadways, the large negative areas vary spatially because of day-to-day changes in wind direction, suggesting daily negative differences (~10 ppb) could be much larger than episode-average MDA8 O_3 reductions (3-4 ppb, in the last panel of Fig. 6). Fig. S7 depicts the simulated base year O_3 during the peak time (13-16 CST) and morning rush hour (6-9 CST), and Fig. S8, the difference plots, illustrate the corresponding changes in future year scenarios. The spatial distribution patterns of the BASE and difference O_3 during the peak time are similar to those of the MDA8 O_3, but with higher magnitudes. During the morning rush hour, however, the average O_3 concentrations increase by ~10 ppb in the CT case, which results from NO_x reductions and less titration (last panel of Fig. S8). The morning O_3 increase due to NO_x reduction is also reported by the study of vehicle electrification over the Yangtze River Delta region in China by Ke et al. (2017).

3.3.2. $PM_{2.5}$ and speciated $PM_{2.5}$

$PM_{2.5}$ comprises a large number of species which widely differ in properties. Table S5 lists the primary $PM_{2.5}$ species represented in the SMOKE and CMAQ models. Fig. S9 displays the composition of domain-wide CMAQ simulated ground-level $PM_{2.5}$ species. The sum of inorganic aerosols (sulfate, nitrate, and ammonium) accounts for 30%, with sulfate being predominant (23%). The sum of primary organic carbon (POC), secondary organic carbon (SOC), elemental carbon (EC), and primary non-carbon mass (APNCOM) constitute 25% of simulated ground-level $PM_{2.5}$ species. Sodium (Na^+), chloride (Cl^-), and trace metals (Fe, Al, Si, Ti, Ca^{2+}, Mg^{2+}, K^+, Mn) occupy 15% in total, with the remaining unspeciated $PM_{2.5}$ accounting for 30%. Simulated concentrations of $PM_{2.5}$ and its major speciated components are plotted in Fig. 7 for September 2013. Total $PM_{2.5}$ concentrations in most regions fall below 20 μg m^{-3}, except over industrial locations with large clusters of petrochemical and chemical manufacturing facilities. Relatively high concentrations of POC, APNCOM, and EC are predicted over highways, representing significant emissions from both gasoline and diesel motor vehicles, as corroborated by previous studies (e.g. Lane et al., 2007; Roy et al., 2011). SOC includes secondary products from both anthropogenic and biogenic sources (Carlton et al., 2010). Their hotspots are located over forest areas, indicating oxidation of biogenic VOCs (e.g., isoprene and monoterpenes) and aged biogenic aerosols are the major contributors. Elevated sulfate and ammonium concentrations are predicted near industrial sources. Sulfate contributions are likely due to the burning of sulfur-containing fuels in the Houston Ship Channel and from coal-fired power plants (Zhang et al., 2015). Shimadera et al. (2014) suggested that nitrate can be affected by ammonia (NH_3) concentrations and the formation of ammonium nitrate (NH_4NO_3).

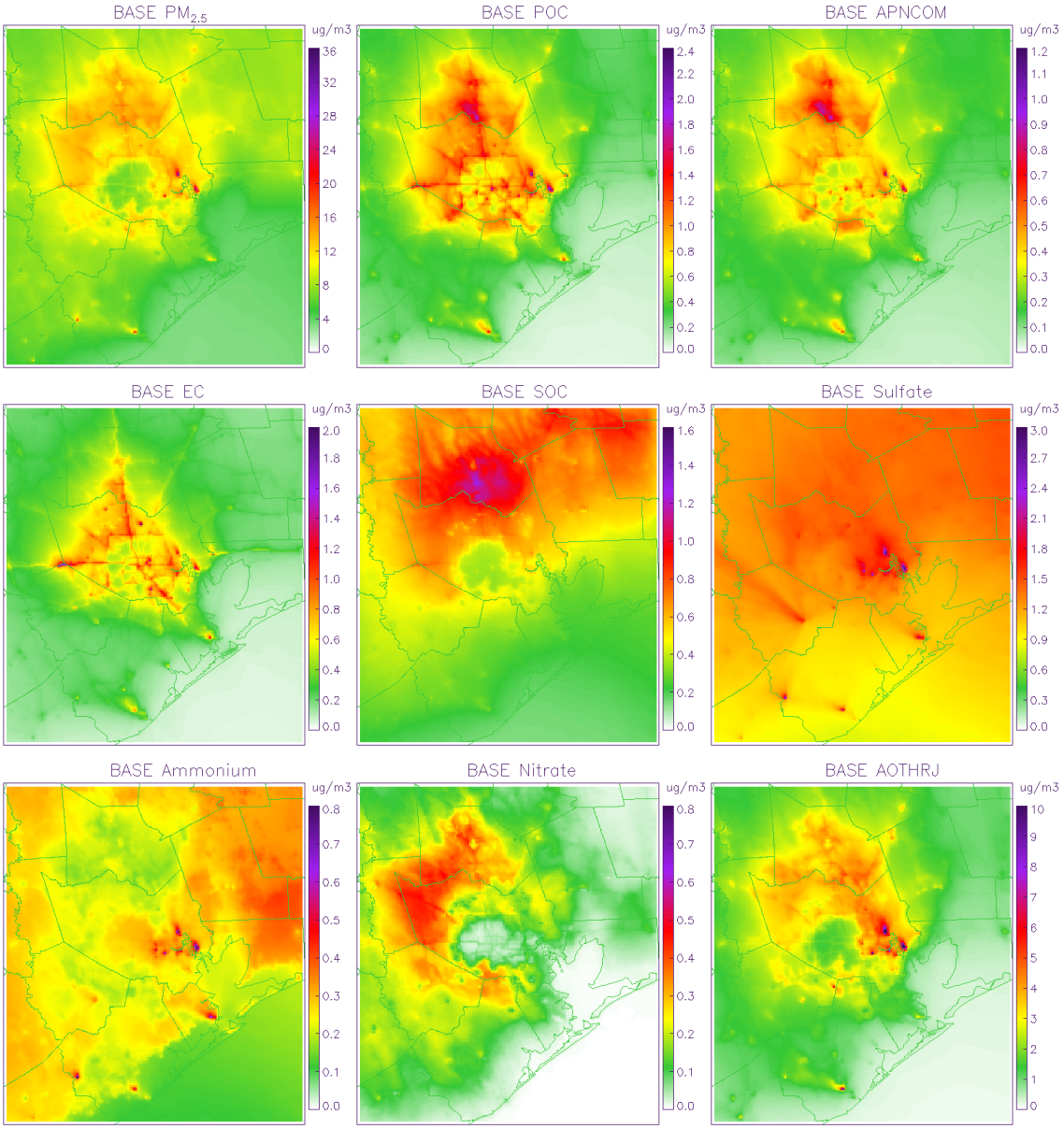

Fig. 7. Spatial distributions of surface concentrations of monthly average $PM_{2.5}$ and major speciated $PM_{2.5}$ during September 2013 in the BASE case. (Acronyms: POC - primary organic carbon; APNCOM - primary non-carbon mass; EC - elemental carbon; SOC - secondary organic carbon; AOTHRJ - other unspeciated species).

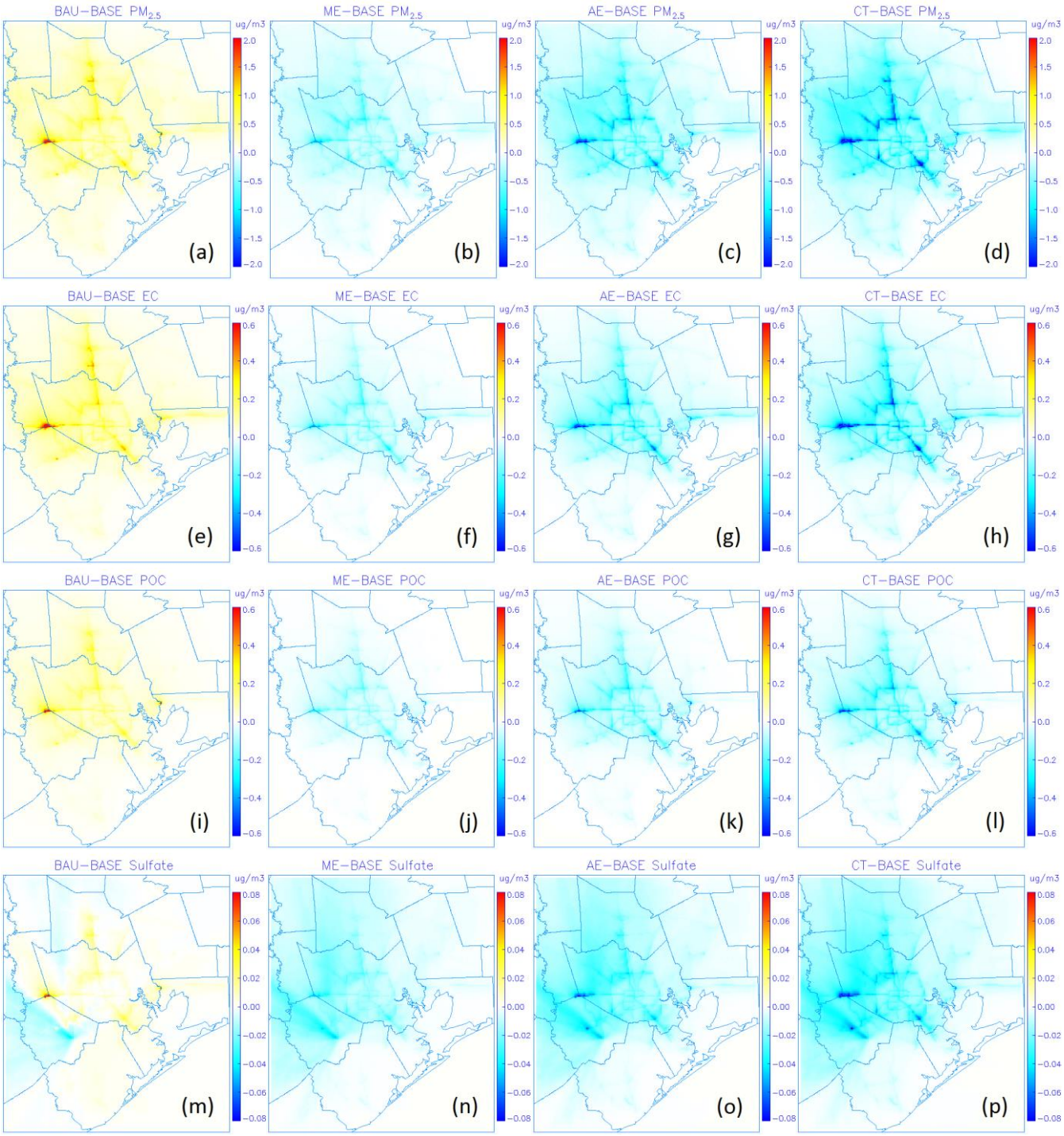

Fig. 8. The spatial difference of surface concentrations of monthly average total $PM_{2.5}$, EC, POC, and sulfate between different simulations: BAU-BASE; ME-BASE; AE-BASE, and CT-BASE.

Because of the changes in mobile $PM_{2.5}$ emissions in the future year cases, understanding the major species that make up mobile emissions is useful and important. The SPECIATE databases (U.S. EPA, 2017a) have reported that elemental carbon (EC) and organic carbon (OC) have high weight fractions for $PM_{2.5}$ speciation in transportation sources, such as Heavy Duty Diesel Vehicles (HDDV)

exhaust (EC: 77%; OC: 17.5%), Light Duty Diesel Vehicles (LDDV) exhaust (EC: 51.4%; OC: 35.5%), and on-road gasoline exhaust (EC: 19%; OC: 55%). Here, we calculated the mass fraction of each $PM_{2.5}$ component in the aggregated on-road mobile emissions in Table S6. Species with higher fractions will undergo a relatively substantial change in the future year cases, as opposed to those with lower fractions. Similarly, the two biggest components of $PM_{2.5}$ are elemental carbon (42%) and primary organic carbon (30%). Thus, the changes in total $PM_{2.5}$ concentrations are mainly associated with changes in carbonaceous species. Fig. 8 plots the differences between the projected scenarios and the base 2013 case. Panels (a)-(d) represent total $PM_{2.5}$ concentrations. The BAU case results in an increase in $PM_{2.5}$ concentrations of 1-2 $\mu g\ m^{-3}$, while the control scenarios show decreases in $PM_{2.5}$ concentrations ranging from 0.5-2 $\mu g\ m^{-3}$. The most dramatic changes occur on highways because of reductions in motor vehicle emissions, corroborated in the plots for EC (panels (e)-(h)) and POC (panels (i)-(l)). The changes in sulfate also mirror those of EC and POC, but one additional important point is the reduction in sulfate hotspots over regions with EGU emissions, due to the reduction in coal capacity over these areas. The changes in $PM_{2.5}$ concentrations could also be attributable to other chemical reactions associated with gas-to-particle conversion (e.g., $HNO_3(g) \rightarrow$nitrate). In all the control scenarios, the reduced NO_x, a precursor for HNO_3, contributed to the decreased nitrate concentrations over the downwind northwest (Fig. S10). Moreover, the decreased VOCs emissions in the urban area also lead to reduction in the concentrations of secondary organic carbon.

3.4. Evaluation of the changes in health endpoints and benefits

The health impact calculations in BenMAP are based on concentration-response (C-R) functions, which represent a decrease in health incidence with air pollutant concentrations. Based on these calculations, the BAU case would likely result in an increased number of premature deaths with respect to 2013. All of the control scenarios, however, would result in prevented mortality, as shown in Table 4. For $PM_{2.5}$, the table shows about 121 more premature deaths in the BAU case over greater Houston, and 109, 177, and 229 prevented premature deaths in the ME, AE, and CT cases, respectively. These findings coincide with trends in $PM_{2.5}$ concentration, as depicted in panels (a)-(d) in Fig. 8. The findings also roughly correspond to a 61% increase in $PM_{2.5}$ emissions in the BAU case, and 46%, 75%, and 95% reductions in the ME, AE, and CT cases listed in Table S4.

Interpreting the O_3 results, however, is more complicated because the trends of O_3 change vary spatially (panels (m)-(p) of Fig. 6). For instance, in the BAU case, BenMAP predicts an increase in adverse health effects over downwind areas because of O_3 increases, while predicting a decrease of damage in the urban and major highways. The net number of premature deaths is negligible at -0.04, and indicates that the downwind negative impact is barely larger than the positive impacts in the urban area. In contrast, for the other scenarios with emissions reductions (i.e., the ME, AE, and CT cases), the gains in health endpoints in downwind areas are all greater than the losses over the urban highways, resulting in about 5, 11, and 17 prevented premature deaths, respectively. We may expect more health benefits if the simulation domain were to cover more downwind areas. It should be noted that even in the case of an increase in O_3 concentrations over the urban highways, reductions in air toxics emissions would occur, which would lead to more health benefits not studied here because the health impact functions for

these air toxics are not available in the current BenMAP model. The economic cost (benefit) values generally coincide with premature mortality results.

Table 4. Estimates of avoided premature mortality and benefits from the changes in O_3 and $PM_{2.5}$ concentrations in the future year scenarios, over the entire study domain.

Species	Scenarios	Premature Mortality Prevented	Benefits [Million Dollars, in 2015 currency year]
Ozone	Business As Usual	-0.04	-0.33
Ozone	Moderate Electrification	5	44
Ozone	Aggressive Electrification	11	97
Ozone	Complete Turnover	17	152
$PM_{2.5}$	Business As Usual	-122	-1,058
$PM_{2.5}$	Moderate Electrification	109	948
$PM_{2.5}$	Aggressive Electrification	177	1,542
$PM_{2.5}$	Complete Turnover	229	1,993

Notation: (1) The age range is 0 to 99 for O_3 and 30 to 99 for $PM_{2.5}$. (2) In the 3rd and 4th columns, positive values indicate the number of premature deaths prevented because of control strategies and the associated benefits achieved, while the negative values in the BAU case indicate an increase in the number of premature deaths and economic losses.

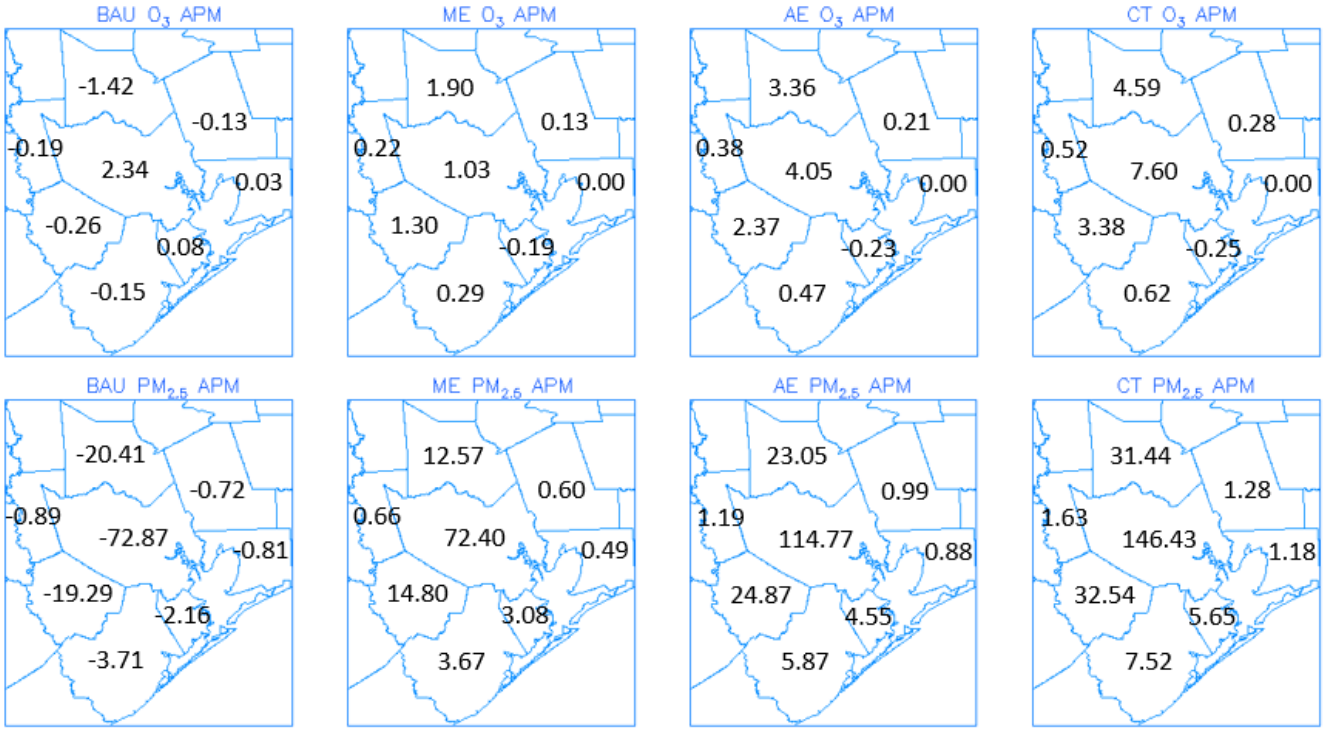

Fig. 9. The county-level avoided premature mortality (APM) resulting from the changes in O_3 and $PM_{2.5}$ concentrations in the future year scenarios.

Fig. 9 plots the county-level avoided premature mortality results. For $PM_{2.5}$, among all the counties, Harris County (in the middle) exhibits significant larger changes due to its high population and dominant change in $PM_{2.5}$ concentrations. For O_3, the net increase of avoided premature mortality in Harris County in BAU case (2.34) are contributed by O_3 reduction over highways, while those in the control cases (1.03, 4.05, and 7.60) result from the O_3 reduction over the outflow regions, as

corroborated in panels (m)-(p) of Fig. 6. Table 5 shows similar trends in O_3-induced morbidities and associated benefits. Thus, the emission reduction scenarios would significantly reduce asthma exacerbation and school loss days, benefiting younger individuals.

Table 5. Estimates of prevented O_3-induced morbidities and benefits in the future year scenarios.

Scenarios	Asthma exacerbation, one or more symptoms	Benefits [Million Dollars, in 2015 currency year]
Business As Usual	-1,213	-0.076
Moderate Electrification	7,534	0.475
Aggressive Electrification	16,119	1.016
Complete Turnover	24,652	1.554
	Emergency room visits, Asthma	
Business As Usual	-0.96	-0.001
Moderate Electrification	20	0.010
Aggressive Electrification	43	0.023
Complete Turnover	67	0.036
	School loss days	
Business As Usual	-833	-0.088
Moderate Electrification	5,518	0.585
Aggressive Electrification	11,844	1.255
Complete Turnover	18,153	1.924
	Hospital admission, All respiratory	
Business As Usual	-0.05	-0.002
Moderate Electrification	4	0.133
Aggressive Electrification	8	0.294
Complete Turnover	13	0.459

Notation: Positive values indicate the number of prevented morbidities and benefits achieved, while the negative values indicate an increase in the number of morbidities and economic losses.

4. Conclusions and discussion

This study modeled multiple scenarios to investigate the effects of control technologies, fleet turnover, and electrification of both gasoline and diesel vehicles on air quality and health over the eight-county O_3 nonattainment region around Houston in the year 2040. Comparing scenarios for the year 2040 to the base year of 2013, we found that emissions increased by ~50% emissions in the BAU case, and they reduced by ~50%, ~75%, and ~95% in the ME, AE, and CT cases, respectively. These numbers held true for all criteria pollutants and VOCs (including air toxics).

The BAU case represented increased emissions with no controls. Consequently, for this case, the CMAQ-simulated O_3 concentrations along highways decreased because of NO_x-titration. However, they resulted in the significant O_3 formation in the NO_x-limited outflow bordering the highway loop in Houston. The emissions control cases all resulted in O_3 increases along the highways because of decreasing NO_x saturation. However, they resulted in an O_3 reduction in both regions enclosed by the highways and those in outflow areas. Simulated $PM_{2.5}$ concentrations showed elemental and organic carbon hotspots along the highways, the magnitudes of which decreased with increasing control and

fleet turnover. One important point was the removal of sulfate hotspots in 2040 resulting from the retirement of coal-fired EGU use. For the assessment of the health impact resulting from the change in O_3 and $PM_{2.5}$ concentrations, we found that the BAU case would lead to 122 additional premature deaths, while the ME, AE, and CT cases would prevent 114, 188, and 246 premature deaths, respectively. In addition, the prevented morbidities and economic cost (benefit) values generally mirrored premature mortality. Our analyses of the Houston Metropolitan area can shed light on the effects of mobile emissions control strategies in other coastal urban environments. Large urban cities can benefit significantly from reductions in $PM_{2.5}$ pollution if local emissions from the transportation sector are controlled, while efficient O_3 pollution reductions primarily occur in downwind areas.

The BAU case, with no change in emission factors, is technically not real since newly manufactured vehicles will follow the current latest emission standards, which are usually more stringent than previous standards. In addition, several state policies have implemented retrofitting (e.g. CARB, 2014; TCEQ, 2017) currently in place. These initiatives will result in reduction in future emission factors. In the other sense, the BAU case can represent revoking of advanced emissions standards and control policies, and hence, the "worst case" scenario. In terms of O_3 pollution, the BAU case would not significantly change the aggregated numbers of premature mortality, but still have substantial impact on minor effects such as asthma exacerbation and school loss days. The CT case, assuming a fully turnover of the current fleet, will not be easy and require a range of strong policies. For example, current age distributions of vehicles vary by source type but almost all source types occupy notable fractions between 20 and 30 years (U.S. EPA, 2015c). Some heavy-duty trucks last more than 30 years and may turn from normal to high emitters (Liu et al., 2015). Hence, the BAU and CT cases are two extreme conditions. The actual future would be close to what exhibited in the ME case or close to those in the AE case with a stronger policy promoting electrification.

Borkar et al. (2016) indicated significant retirement of fossil capacity and marked replacement of fossil fuel sources by renewables for the Houston eight-county area. The retirement of coal-fired power plants could provide an impetus to clean electrification in Texas; these efforts, however, might not be replicable everywhere. For example, according to the Emissions and Generation Resource Integrated Database (eGRID) (U.S. EPA, 2017c), about 67% of energy generation in the state of Ohio in the year 2014 was by coal, and the added load due to electrification could exacerbate an existing nonattainment problem. Hence, to gain a more comprehensive understanding of the overall effects of fleet electrification and the long-range transport of emissions outside of Houston and Texas, we would have to investigate several scenarios throughout the continental United States. It is also interesting to see how aggressive electrification would impact the air quality and health in the national level.

There are several limitations and uncertainties associated with this study. One important limitation is that a detailed microscopic traffic assessment and geodemographic (population density, transportation mode, land use) analysis is not included/fully considered in this study. For instance, the projected future mobile activity data provided by TTI are county- and vehicle type- specific, while the advent of autonomous vehicles has the potential to dramatically change the current transportation systems. Shared autonomous vehicles are expected to reduce travel distance and vehicle ownership,

impacting on land use (e.g., parking infrastructure) and travel patterns (Shaheen and Cohen, 2013; Fagnant and Kockelman, 2014). Hence, the diurnal and spatial patterns of mobile emissions may also change. In addition, the population growth rates in the health impact model are at county-level, while the distribution of population could possibly change within each county. In this study, we made projections for on-road mobile and EGUs sectors, the emissions for other sectors were fixed to present levels. The meteorological conditions and chemical boundaries were also kept unchanged. These would affect the future total air quality levels (Bell et al., 2007a; 2007b). Another uncertainty is that we applied fixed fractional rates of fleet turnover and control factor. The actual vehicle fleet composition may vary in the future and largely depend on policy, pricing, and technology. But the future emissions should fall between our four scenarios here. Also if technologies are not ready in 2040 to reduce non-exhaust emissions (e.g., $PM_{2.5}$ emissions from brake and tire wear) from electric fleet, the corresponding change in $PM_{2.5}$ concentrations and health outcomes would likely be smaller than the numbers reported in this study.

In the health impact analysis, the C-R relationships are derived from long-term air quality measurements and health records data, while only one month simulations were used here because the 1×1 km simulations were too computational expensive. Hence the health impact results may be over- or under- estimated if seasonal variation of air pollutants concentrations are considered. In addition, the uncertainties in emissions may impact the air quality and health outcomes. For instance, McDonald et al. (2018) reported the over-prediction of NO_x mobile emissions in the National Emission Inventory. In our study, if the NO_x mobile emissions are over-predicted in the base case, then the change in NO_x emissions or concentrations between the base and future year cases would be smaller than the numbers reported in this study, resulting potential less change in O_3 concentrations and subsequent over-prediction of the health outcomes. While also as suggested by McDonald et al. (2018), reduction in mobile source NO_x emissions could help reducing the number of high O_3 days in the Eastern U.S. and meeting more stringent O_3 standards in the future. In our cases, the fleet electrification could possibly lead to less emissions accumulation during the meteorological conditions favoring O_3 production (e.g., land-bay/sea breeze recirculation, early morning low wind speeds), and potential less events of O_3 exceedance. Overall, this study provides proof-of-concept of how the combined effects of a greening grid, emissions control, and fleet electrification can improve air quality and human health.

Acknowledgements

The authors acknowledge the support from the U.S. Department of Transportation (DOT) Center for Transportation, Environment, and Community Health (CTECH). The authors thank the contributions from Anirban Roy, Yunsoo Choi, and Ebrahim Eslami (University of Houston), Stephanie Thomas and Thomas Smith (Public Citizen), Xiangyu Jiang (University at Buffalo), Dennis Perkinson (Texas Transportation Institute), and Warren Lasher (Electric Reliability Council of Texas).

Supplemental Information

S1. A simplified flow chart of the air quality modeling system

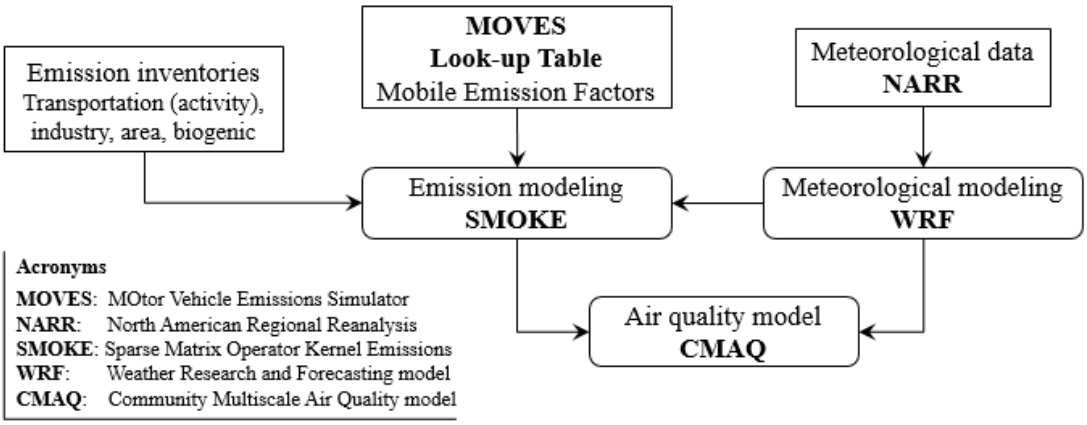

Fig. S1. A simplified flow chart of the air quality modeling system.

S2. Calculations of electricity demand

S2.1. Fleet turnover with new and electric vehicles

This calculation was performed for the Aggressive Electrification scenario, which represents the highest electricity consumption for electric and hybrid vehicles and hence provides bounding estimates. The VMT data were fractionated into New, Electric, and Current types.

For light-duty "New" vehicles, we assume new technologies will all be hybrid, since major automobile manufacturers such as Volvo and Jaguar-Land Rover have already announced plans to build only hybrid vehicles post-2020. The United States Department of Energy (U.S. DOE)'s Energy Information Administration (EIA)'s Annual Energy Outlook of 2018 (AEO2018) provides the categories of hybrid (HEV), plug-in hybrid (PHEV), and all-electric vehicles (BEV) differing in range. According to the report, the proportion of electric vehicles with all-electric range (AER) 100, 200 and 300 in 2040 was projected to be 1:5:5 roughly, translating into overall fractions of 0.0636, 0.318 and 0.318 respectively (adding up to 0.7 that represents total "Electric" fraction). Similarly, the ratio of standard to plug-in hybrids was projected by the AEO to be roughly 3:1, resulting in 0.116 of hybrid and 0.034 of plug-in hybrid (adding up to 0.15 that represents total "New" fraction). The Argonne National Laboratory's Autonomie data further indicate PHEVs will be of four types, namely PHEV10, PHEV20, PHEV30 and PHEV40. In the absence of information, each of these assumed to have an equal share.

For heavy-duty diesel vehicles, in absence of adequate information on hybrid projections, we assume all new vehicles to be electric vehicles, resulting in 85% of electric vehicles in 2040.

S2.2. Energy consumption for hybrid and electric vehicles

Projections for electricity consumption (Wh mile^{-1}) were taken from the Argonne National Laboratory's Autonomie model output (https://www.autonomie.net/). Their modeling involves projections all the way to 2040. The assumption is that a typical vehicle technology takes 5 years to reach the market once conceived in the laboratory. Hence, a laboratory year of 2035 is needed if we are considering a 2040 model year. A sample projection is illustrated in Fig. S2 for electricity consumption, indicating a linear trend from 2030 to 2045. Hence, the number for 2035 can be approximated linearly. Autonomie data covers the following vehicle classes: compact, midsize, small SUV, midsize SUV, pick-up truck. These were mapped to MOVES categories as in Table S1 for electricity consumption per mile (Table S2). Autonomie considered three scenarios based on technology, this study considers the Medium case.

Since data for trucks were not available in Autonomie, these were taken from the Argonne National Laboratory's Alternative Fuel Life-Cycle Environmental and Economic Transportation (AFLEET) model (Burnham, 2017). The AFLEET data were reported originally in diesel-gallon equivalents, which were converted to Wh mi^{-1} using the assumption that one diesel gallon contains 145 MJ, and 0.2778 kWh are contained in 1 MJ, as illustrated by the U.S. DOE EIA's online calculator: (https://www.eia.gov/energyexplained/index.php?page=about_energy_conversion_calculator#dieselcalc). The numbers are listed in Table S3.

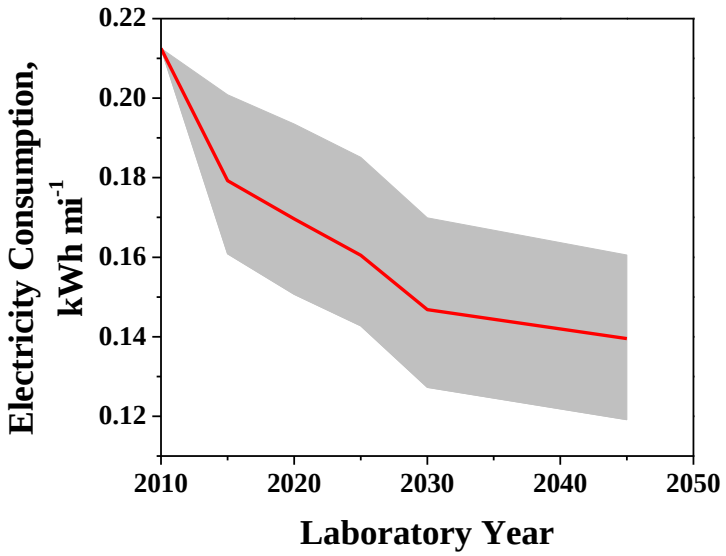

Fig. S2. Sample Autonomie projections for electricity consumption, for a compact battery electric vehicle, AER 100 miles, UDDS testing cycle.

Table S1: Autonomie to MOVES mapping.

Autonomie	Autonomie	MOVES	Conversion
Compact	Midsize	Passenger car	Passenger Car=0.5(Compact+Midsize)
Small SUV	Midsize SUV	Passenger truck	Passenger truck=0.5(Small+Midsize)
Pick-up truck		Light Commercial truck	Light Commercial truck= Pick-up truck

Table S2: Energy consumption for light-duty vehicles, Wh mi^{-1}.

MOVES category	Fuel	Hybrid type	Small	Midsize	Average
Passenger Car	gasoline	PHEV10	36.00	38.49	37.25
Passenger Car	gasoline	PHEV20	62.08	66.41	64.24
Passenger Car	gasoline	PHEV30	79.73	84.63	82.18
Passenger Car	gasoline	PHEV40	94.67	98.98	96.82
Passenger Car	electric	BEV100	212.18	221.88	217.03
Passenger Car	electric	BEV200	217.19	227.30	222.24
Passenger Car	electric	BEV300	232.87	244.70	238.79
Passenger Car	diesel	PHEV10	39.15	41.70	40.43
Passenger Car	diesel	PHEV20	67.56	72.44	70.00
Passenger Car	diesel	PHEV30	82.53	87.37	84.95
Passenger Car	diesel	PHEV40	97.58	102.43	100.00
Passenger truck	gasoline	PHEV10	47.87	55.53	51.70
Passenger truck	gasoline	PHEV20	83.56	93.82	88.69
Passenger truck	gasoline	PHEV30	103.84	119.13	111.49
Passenger truck	gasoline	PHEV40	122.11	142.51	132.31
Passenger truck	electric	BEV100	286.37	337.02	311.69
Passenger truck	electric	BEV200	293.06	346.13	319.60
Passenger truck	electric	BEV300	312.36	366.69	339.52
Passenger truck	diesel	PHEV10	51.21	58.35	54.78
Passenger truck	diesel	PHEV20	88.43	99.67	94.05
Passenger truck	diesel	PHEV30	105.93	121.72	113.83
Passenger truck	diesel	PHEV40	125.34	145.95	135.65
Light Commercial Truck	gasoline	PHEV10	66.84	n/a	n/a
Light Commercial Truck	gasoline	PHEV20	111.94	n/a	n/a
Light Commercial Truck	gasoline	PHEV30	140.89	n/a	n/a
Light Commercial Truck	gasoline	PHEV40	167.51	n/a	n/a
Light Commercial Truck	electric	BEV100	404.47	n/a	n/a
Light Commercial Truck	electric	BEV200	416.19	n/a	n/a
Light Commercial Truck	electric	BEV300	441.40	n/a	n/a
Light Commercial Truck	diesel	PHEV10	69.53	n/a	n/a
Light Commercial Truck	diesel	PHEV20	117.98	n/a	n/a
Light Commercial Truck	diesel	PHEV30	143.16	n/a	n/a
Light Commercial Truck	diesel	PHEV40	170.95	n/a	n/a

Table S3: Energy consumption data for trucks.

AFLEET category	MOVES category	MPG	GPM	MJ/G	MJ/mi	kWh/MJ	kWh/mi
Long Haul Freight Truck	Combination Long-Haul Truck	16.1	0.062	145	9.0	0.28	2.5
Regional Haul Freight Truck	Combination Short-Haul Truck	16.3	0.060	145	8.9	0.28	2.47
Delivery Straight Truck	Single Unit Long-Haul Truck	14.5	0.069	145	10.0	0.28	2. 8
Delivery Step Van	Single Unit Short-Haul Truck	16.3	0.061	145	8.9	0.28	2.47
Refuse Truck	Refuse Truck	3.8	0.260	145	38.16	0.28	10.6
Transit Bus	Transit Bus	9.1	0.110	145	15.93	0.28	4.43
School Bus	School Bus	17.0	0.059	145	8.53	0.28	2.37

S2.3. County-specific electricity demand

The calculation is illustrated with a simple example. For a given vehicle type (e.g. gasoline passenger car), the projected total VMT over the 8-county area is 1.5×10^8 miles in 2040. This is fractionated according to the distributions in Section S1.1, and multiplied by their respective electricity consumption values in Table S2, to obtain total electricity consumption for gasoline passenger cars. The process was then repeated for other vehicles to obtain a total.

We then summed over gasoline and diesel to get a total electricity consumption, which is 6.3×10^4 MWh. On comparing these numbers in context, the regional electricity generation over the 8-county area is 7.5×10^7 MWh. Therefore, the electricity requirements for motor vehicles appear to be negligible compared to regional electricity generation. This could be due to that the Autonomie numbers represent improved technology and efficiency in 2040, which result in lowered consumption.

S3. Supplemental results

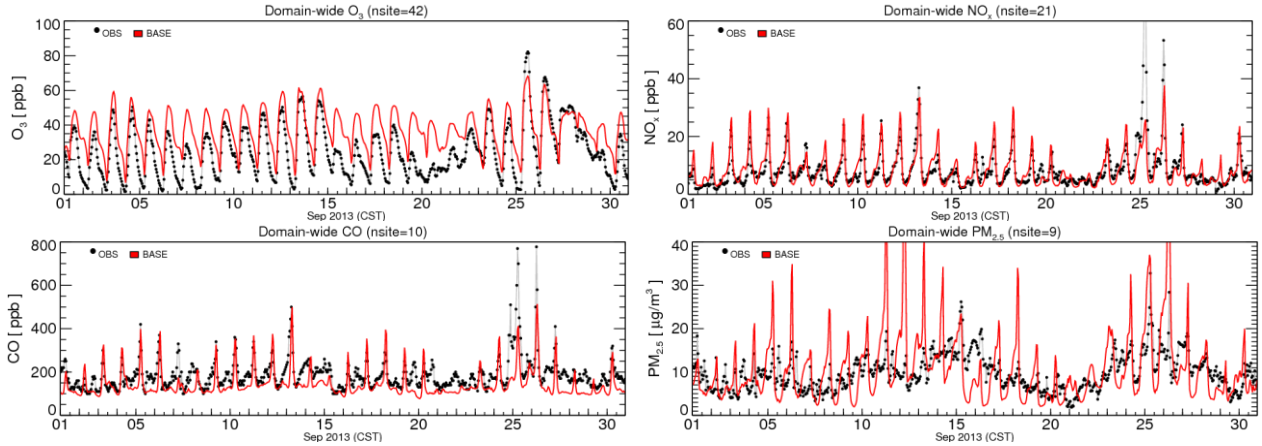

Fig. S3. Time series comparisons of domain-wide surface concentrations of O_3, NO_x, CO, and $PM_{2.5}$ between observations (OBS) and Base year simulation (BASE) during September 2013.

Table S4. Episode-average eight-county aggregated on-road mobile emissions in the BASE case and comparative changes in future scenarios.

Species	BASE [tons day^{-1}]	Differences to BASE [%] Business As Usual	Differences to BASE [%] Moderate Electrification	Differences to BASE [%] Aggressive Electrification	Differences to BASE [%] Complete Turnover
CO	1220.64	48.6	-50.0	-76.6	-95.2
NO_x	207.51	56.9	-47.2	-75.3	-94.9
NH_3	5.51	50.8	-49.2	-76.2	-95.1
SO_2	1.69	50.9	-49.2	-76.2	-95.1
PM_{10}	16.88	55.3	-47.7	-75.5	-94.9
$PM_{2.5}$	6.75	61.1	-45.8	-74.6	-94.8
non-HAP TOG	72.81	48.3	-50.1	-76.6	-95.2
Benzene	2.47	46.3	-50.8	-77.0	-95.2
Formaldehyde	1.66	60.5	-45.8	-74.5	-94.6
Acetaldehyde	1.15	54.3	-48.0	-75.7	-94.9
Acrolein	0.11	63.1	-45.1	-74.3	-94.7
1,3-butadiene	0.44	46.5	-50.7	-76.9	-95.2
Naphthalene	0.21	58.1	-46.8	-75.1	-94.9
N_2O	3.19	44.5	-51.4	-77.2	-95.3
CO_2	92967.76	52.4	-48.7	-76.0	-95.0
CH_4	3.33	54.0	-46.8	-73.9	-92.9

Notation: non-HAP TOG denotes for non-Hazardous Air Pollutant Total Organic Gases. Values in 3rd - 6th columns are in %.

Species Code	Species description
ALD2	Acetaldehyde
ALDX	Propionaldehyde and higher aldehydes
CH4	Methane
ETH	Ethylene
ETHA	Ethane
ETOH	Ethanol
FORM	Formaldehyde
IOLE	Internal olefin carbon bond (R-C=C-R)
ISOP	Isoprene
MEOH	Methanol
OLE	Terminal olefin carbon bond (R-C=C)
PAR	Paraffin carbon bond (C-C)
TERP	Terpenes
TOL	Toluene and other monoalkyl aromatics
UNK	Unknown compounds
UNR	Unreactive compounds
XYL	Xylene and other polyalkyl aromatics

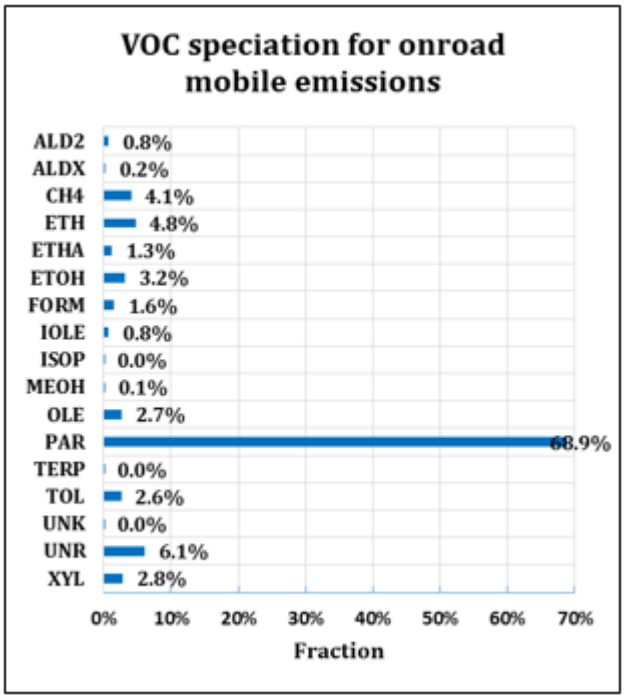

Fig. S4. The left is the description of the VOC species in the CB05 chemical mechanism (Yarwood et al. 2005). The right is averaged VOC speciation (in mole fraction) from on-road mobile emissions for the 8-county area, BASE Case.

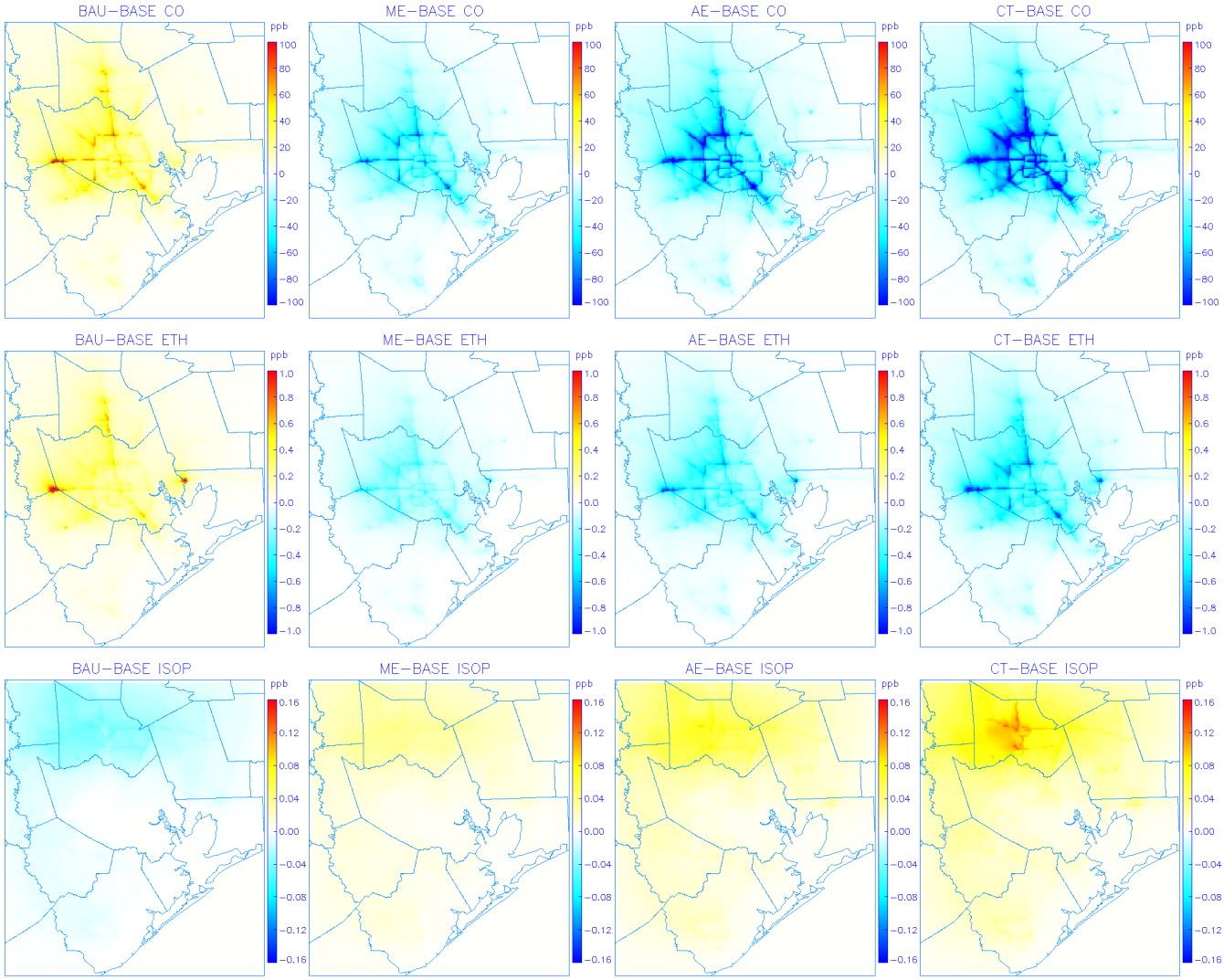

Fig. S5. Spatial difference plots of episode-average surface concentrations of CO, ethylene, and isoprene between different simulations: BAU-BASE; ME-BASE; AE-BASE, and CT-BASE.

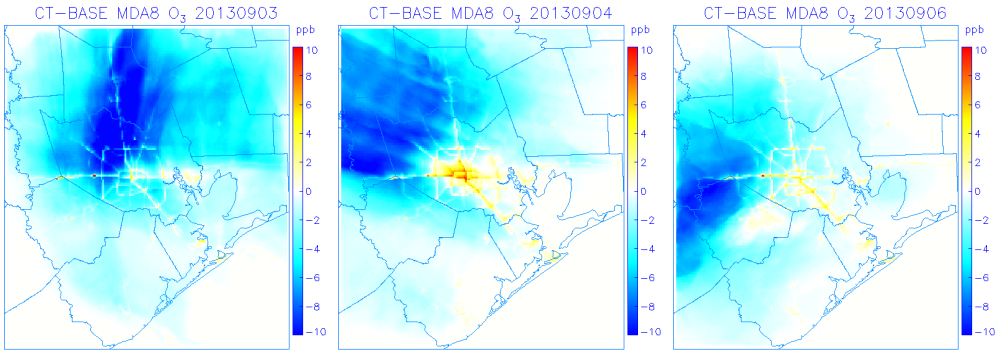

Fig. S6. Select daily MDA8 O_3 difference between the CT case and BASE case (CT minus BASE).

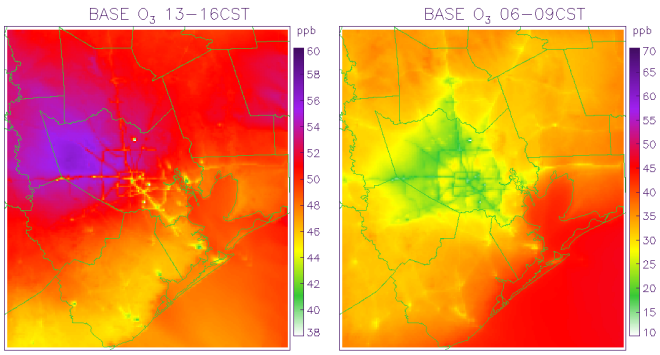

Fig. S7. Simulated O_3 concentrations in the BASE case during peak hour (13-16 CST, left panel) and morning rush hour (6-9 CST, right panel).

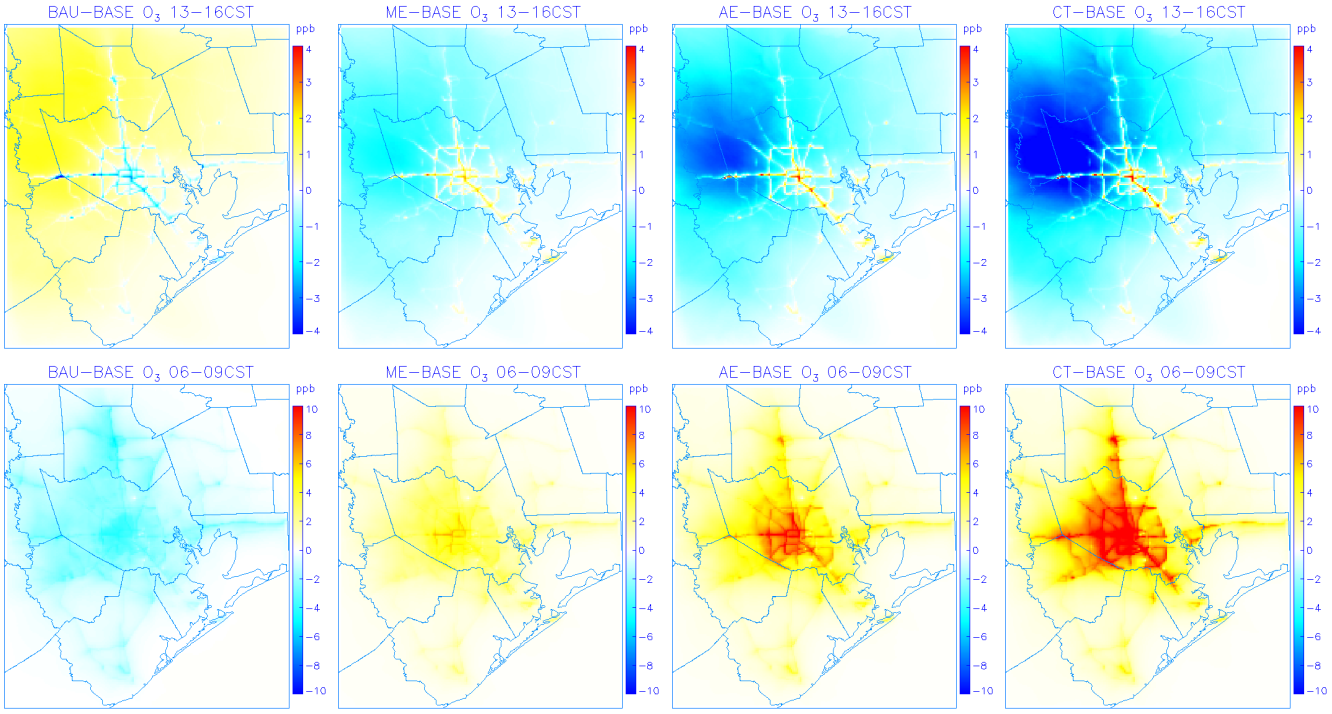

Fig. S8. Simulated O_3 differences during peak time (13-16 CST) and morning rush hour (6-9 CST).

Table S5. Description of speciated $PM_{2.5}$ in the SMOKE and CMAQ models. For the CMAQ species, the suffixes I and J represent Aitken and Accumulation modes, respectively.

SMOKE species	CMAQ species	Species description
PSO4	ASO4 = ASO4I + ASO4J	Sulfate
PNO3	ANO3 = ANO3I+ ANO3J	Nitrate
PNH4	ANH4 = ANH4I + ANH4J	Ammonium
POC	POC = APOCI + APOCJ	Primary organic carbon
	SOC	Secondary organic carbon
PEC	EC = AECI + AECJ	Elemental carbon
PNCOM	APNCOM = APNCOMI + APNCOMJ	Primary non-carbon organic mass
PFE	AFEJ	Iron
PAL	AALJ	Aluminum
PSI	ASIJ	Silica
PTI	ATIJ	Titanium
PCA	ACAJ	Calcium
PMG	AMGJ	Magnesium
PK	AKJ	Potassium
PMN	AMNJ	Manganese
PNA	ANAJ	Sodium
PCL	ACLIJ = ACLI + ACLJ	Chloride
PMOTHR	AOTHRJ	other species

Notation: In 2nd column, the SOC calculation is based on Carlton et al., 2010.

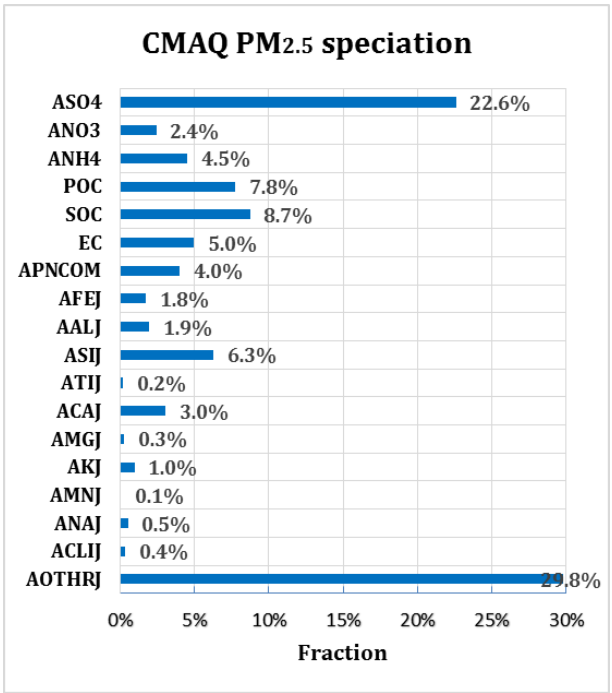

Fig. S9. Domain-wide CMAQ simulated $PM_{2.5}$ speciation (mass fraction) in the model surface layer.

Table S6. Speciation of the aggregated on-road mobile $PM_{2.5}$ emissions.

Species	BASE [g/day]	BASE Mass Fraction
PEC	2.56×10^{6}	41.96%
POC	1.85×10^{6}	30.27%
PMOTHR	6.02×10^{5}	9.86%
PNCOM	4.16×10^{5}	6.81%
PSO4	1.49×10^{5}	2.43%
PFE	1.47×10^{5}	2.40%
PMG	1.17×10^{5}	1.92%
PSI	1.09×10^{5}	1.79%
PNH4	5.28×10^{4}	0.86%
PCA	4.83×10^{4}	0.79%
PNO3	1.99×10^{4}	0.33%
PCL	1.37×10^{4}	0.22%
PAL	8.27×10^{3}	0.14%
PTI	4.72×10^{3}	0.08%
PNA	4.18×10^{3}	0.07%
PK	2.98×10^{3}	0.05%
PMN	1.36×10^{3}	0.02%

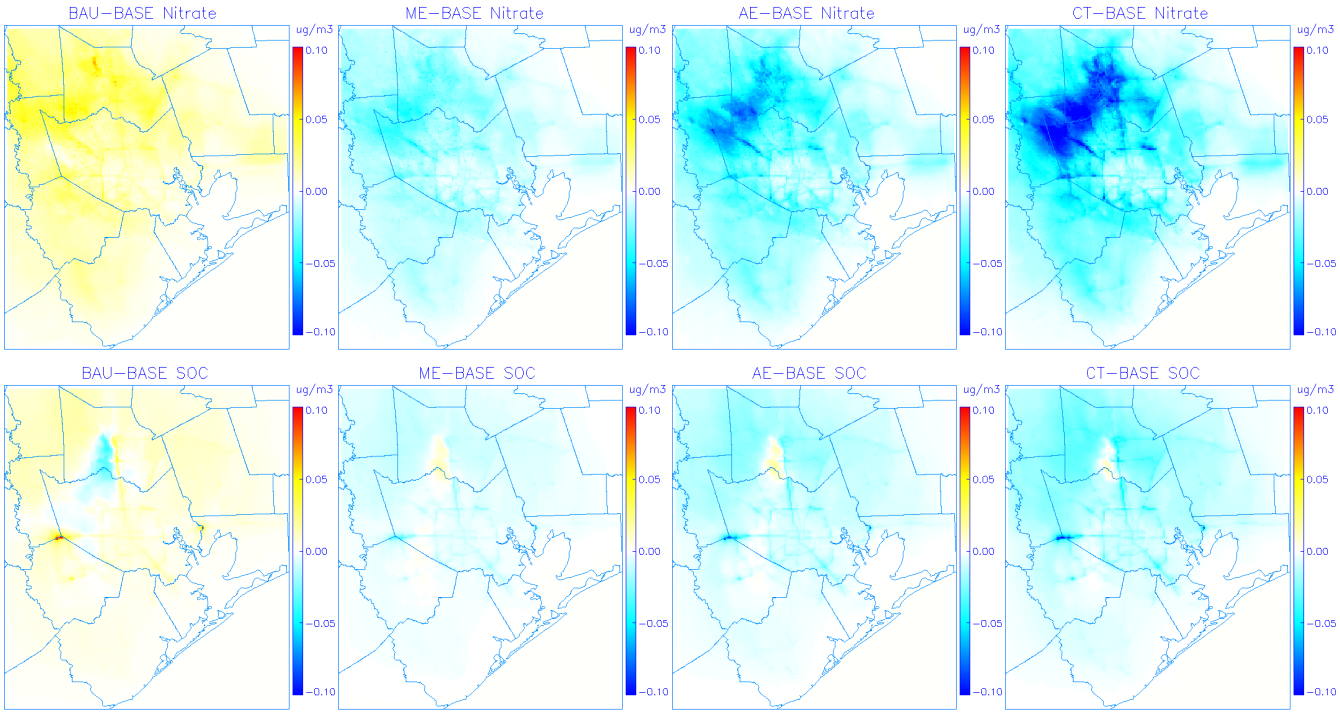

Fig. S10. Spatial difference plots of episode-average surface concentrations of Nitrate and SOC between different simulations: BAU-BASE; ME-BASE; AE-BASE, and CT-BASE.

References

Bell, M. L., Dominici, F., Samet, J. M., 2005. A meta-analysis of time-series studies of ozone and mortality with comparison to the national morbidity, mortality, and air pollution study. Epidemiology, 16(4), 436-45.

Bell, M. L., Dominici, F., Ebisu, K., Zeger, S. L., Samet, J. M., 2007a. Spatial and temporal variation in $PM_{2.5}$ chemical composition in the United States for health effects studies. Environ. Health Perspect., 115(7), 989-995.

Bell, M.L., Goldberg, R., Hogrefe, C., Kinney, P.L., Knowlton, K., Lynn, B., Rosenthal, J., Rosenzweig, C., Patz, J., 2007b. Climate change, ambient ozone, and health in 50 US cities. Climatic Change, 82, 61-76.

BNEF, 2016. Electric vehicles to be 35% of global new car sales by 2040. https://about.bnef.com/blog/electric-vehicles-to-be-35-of-global-new-car-sales-by-2040/

BNEF, 2017. The EV bandwagon is acceleration, but is it unstoppable? https://about.bnef.com/blog/cheung-ev-bandwagon-accelerating-unstoppable/

Brinkman, G., Denholm, P., Hannigan, M. P., Milford, J. B., 2010. Effects of plug-in hybrid electric vehicles on ozone concentrations in Colorado. Environ. Sci. Technol., 44, 6256-6262.

Borkar, S., Opheim, C., Murray, D., Bilo, J., 2016. ERCOT System Planning: 2016 Long-Term System Assessment for the ERCOT Region Version 1.0.

Burnham, 2017. User Guide for AFLEET Tool 2017. https://greet.es.anl.gov/files/afleet-tool-2017-user-guide.

Byun, D., Kim, S., Czader, B., Nowak, D., Stetson, S., Estes, M., 2005. Estimation of biogenic emissions with satellite-derived land use and land cover data for air quality modeling of Houston-Galveston ozone nonattainment area. J. Environ. Manage., 75, 285-301. doi:10.1016/j.jenvman.2004.10.009.

Byun, D. and Schere, K. L., 2006. Review of the governing equations, computational algorithms, and other components of the Models-3 Community Multiscale Air Quality (CMAQ) modeling system, Appl. Mech. Rev., 59, 51–77.

California Air Resources Board (CARB), 2014. Truck and bus regulation: current regulation and advisories. https://www.arb.ca.gov/msprog/onrdiesel/regulation.htm.

Carlton, A. G., Bhave, P. V., Napelenok, S. L., Edney, E. O., Sarwar, G., Pinder, R. W., Pouliot, G. A., Houyoux, M., 2010. Model representation of secondary organic aerosol in CMAQv4.7. Environ. Sci. Technol., 44, 8553-8560.

Chen, L., Jennison, B. L., Yang, W., Omaye, S. T., 2000. Elementary school absenteeism and air pollution. Inhal. Toxicol., 12(11), 997-1016.

Choi, Y., Kim, H., Tong, D., and Lee, P., 2012. Summertime weekly cycles of observed and modeled NO_x and O_3 concentrations as a function of satellite-derived ozone production sensitivity and land use types over the Continental United States, Atmos. Chem. and Phys., 12, 6291-6307.

Choi, Y., Jeon, W., Roy, A., Souri, A., Diao, L., Pan, S., Eslami, E., 2016. CMAQ modeling archive for exceptional events analyses. Texas Comm. on Environ. Quality, Final Report, August 2016, available at https://www.tceq.texas.gov/airquality/airmod/project/pj_report_pm.html.

Diao, L., Choi, Y., Czader, B., Li, X., Pan, S., Roy, A., Souri, A., Estes, M., Jeon, W., 2016. Discrepancies between modeled and observed nocturnal isoprene in an urban environment and the possible causes: A case study in Houston, Atmos. Res., 181, 257-264.

Elgowainy, A., Han, J., Poch, L., Wang, M., Vyas, A., Mahalik, M., Rousseau, A., 2010.Well-to-Wheels Analysis of Energy Use and Greenhouse Gas Emissions of Plug-In Hybrid Electric Vehicles. https://greet.es.anl.gov/publication-xkdaqgyk.

Fagnant, D. J., and Kockelman, K. M., 2014. The travel and environmental implications of shared autonomous vehicles, using agent-based model scenarios. Trans. Res. Part C, 40, 1-13.

Fann, N., Baker, K. R., Fulcher, C. M., 2012. Characterizing the $PM_{2.5}$-related health benefits of emission reductions for 17 industrial, area and mobile emission sectors across the U.S., Environment International, 49, 141-151.

Fann, N., Fulcher, C. M., Baker, K., 2013. The recent and future health burden of air pollution apportioned across US Sectors. Environ. Sci. Technol., 47(8), 3580–3589.

Gilliland, F. D., Berhane, K., Rappaport, E. B., Thomas, D. C., Avol, E., Gauderman, W. J., London, S. J., Margolis, H. G., McConnell, R., Islam, K. T., Peters, J. M., 2001. The effects of ambient air pollution on school absenteeism due to respiratory illness. Epidemiology, 12(1), 43-54.

Glad, J. A., Brink, L. L., Talbott, E. O., Lee, P. C., Xu, X., Saul, M., Rager, J., 2012. The relationship of ambient ozone and PM2.5 levels and asthma emergency department visits: possible influence of gender and ethnicity. Arch. Environ. Occup. Health, 67(2):103-8.

Huo, H., Zhang, Q., Liu, F., He, K., 2013. Climate and environmental effects of electric vehicles versus compressed natural gas vehicles in China: a life-cycle analysis at provincial level. Environ. Sci. Technol., 47, 1711-1718.

Ito, K., Thurston, G. D., Silverman, R. A., 2007. Characterization of $PM_{2.5}$, gaseous pollutants, and meteorological interactions in the context of time-series health effects models. J. Expo. Sci. Environ. Epidemiol., 17 Suppl 2, S45-60.

Ji., S., Cherry, C. R., Bechle, M. J., Wu, Y., Marshall, J. D., 2012. Electric vehicles in China: emissions and health impacts. Environ. Sci. Technol., 46, 2018-2024.

Katsouyanni, K., Samet, J. M., Anderson, H. R., Atkinson, R., Tertre, A. L., Medina, S., et al., 2009. Air pollution and health: A European and North American Approach (APHENA). Health Effects Institute.

Ke, W., Zhang, S., Wu, Y., Zhao, B., Wang, S., Hao, J., 2016. Assessing the future vehicle fleet electrification: the impacts on regional and urban air quality. Environ. Sci. Technol., 51, 1007-1016.

Krewski D, Jerrett M, Burnett R, et al., 2009. Extended follow-up and spatial analysis of the American Cancer Society linking particulate air pollution and mortality. Health Effects Institute, Cambridge, MA.

Lane, T. E., Pinder, R. W., Shrivastava, M., Robinson, A. L., Pandis, S. N., 2007. Source contributions to primary organic aerosol: comparison of the results of a source-resolved model and the chemical mass balance approach. Atmos. Environ., 41, 18, 3758-3776.

Levy, J. I., Chemerynski, S. M., Sarnat, J. A., 2005. Ozone exposure and mortality: an empiric bayes metaregression analysis. Epidemiology, 16(4): 458-68.

Li, N., Chen, J.-P., Tsai, I-C., He, Q., Chi, S.-Y., Lin, Y.-C., Fu, T.-M., 2016. Potential impacts of electric vehicles on air quality in Taiwan. Sci. of the Total Environ., 566-567, 919-928.

Li, X., Choi, Y., Czader, B., Roy, A., Kim, H., Lefer, B., Pan, S., 2016. The impact of observation nudging on simulated meteorology and ozone concentrations during DISCOVER-AQ 2013 Texas campaign. Atmos. Chem. Phys., 16, 3127-3144. doi:10.5194/acp-16-3127-2016.

Liu, L., Hwang, T., Lee, S., Ouyang, Y., Lee, B., Smith, S. J., Yan, F., Daenzer, K., Bond, T. C., 2015. Emission projections for long-haul freight trucks and rail in the United States through 2050. Environ. Sci. Technol., 49,11569-11576.

Loughner, C. P., Follette-Cook, M. B., Fried, A., Pickering, K., Gilliam, R., Mackay, J., 2015. The role of bay breezes on a high surface ozone episode during the Houston, Texas DISCOVER-AQ field campaign, 7th International Workshop on Air Quality Forecasting Research, September 3, 2015, available at http://www.arl.noaa.gov/IWAQFR_Presentations_2015.php.

Mar, T. F., and Koenig, J. Q., 2009. Relationship between visits to emergency departments for asthma and ozone exposure in greater Seattle, Washington. Annals of Allergy, Asthma, and Immunology, 103, 474-479.

McDonald, B. C., McKeen, S. A., Cui, Y. Y., Ahmadov, R., Kim, S.-W., Frost, G. J., Pollack, I. B., Peischl, J., Ryerson, T. B., Holloway, J. S., Graus, M., Warneke, C., Gilman, J. B., de Gouw, J. A., Kaiser, J., Keutsch, F. N., Hanisco, T. F., Wolfe, G. M., Trainer, M., 2018. Modeling ozone in the Eastern U.S. using a fuel-based mobile source emissions inventory. Environ. Sci. Technol., 52, 7360-70.

Mesinger F. et al, NORTH AMERICAN REGIONAL REANALYSIS: A long-term, consistent, high-resolution climate dataset for the North American domain, as a major improvement upon the earlier global reanalysis datasets in both resolution and accuracy, submitted to BAMS 2004. Available at: http://www.esrl.noaa.gov/psd/.

Mortimer, K. M., Neas, L. M., Dockery, D. W., Redline, S., Tager, I. B., 2002. The effect of air pollution on inner-city children with asthma. Eur. Respir. J., 19(4), 699-705.

Nichols, B. G., Kockelman, K. M., Reiter, M., 2015. Air quality impacts of electric vehicle adoption in Texas. Transportation Research Part D, 34, 208-218.

Nopmongcol, U., Grant, J., Knipping, E., Alexander, M., Schurhoff, R., Young, D., Jung, J., Shah, T., Yarwood, G., 2017. Air quality impacts of electrifying vehicles and equipment across the United States. Environ. Sci. Technol., 51, 2830-2837.

O'Connor G. T., Neas, L., et al., 2008. Acute respiratory health effects of air pollution on children with asthma in US inner cities. J. Allergy Clin. Immunol., 121(5), 1133-1139.

Olaguer E. P., Rappenglueck B., Lefer B., Stutz J., Dibb J., Griffin R., Brune B., Shauck M., Buhrg M., Jeffries H., Vizuete W., Pinto J., 2009. Deciphering the role of radical sources during the Second Texas Air Quality Study, J. of the Air and Waste Manage. Assoc., 59, 11, 1258-1277.

Palmer, K., Tate, J. E., Wadud, Z., Nellthorp, J., 2018. Total cost of ownership and market share for hybrid and electric vehicles in the UK, US and Japan. Applied Energy, 209, 108-119.

Pan, S., Choi, Y., Roy, A., Li, X., Jeon, W., Souri, A. H., 2015. Modeling the uncertainty of several VOC and its impact on simulated VOC and ozone in Houston, Texas. Atmos. Environ., 120, 404-416.

Pan, S., Choi, Y., Jeon, W., Roy, A., Westenbarger, D. A., Kim, H. C., 2017a. Impact of high-resolution sea surface temperature, emission spikes and wind on simulated surface ozone in Houston, Texas during a high ozone episode. Atmos. Environ., 152, 362-376.

Pan, S., Choi, Y., Roy, A., Jeon, W., 2017b. Allocating emissions to 4 km and 1 km horizontal spatial resolutions and its impact on simulated NO_x and O_3 in Houston, TX. Atmos. Environ., 164, 398-415.

Peel, J. L., Tolbert, P. E., Klein, M., et al., 2005. Ambient air pollution and respiratory emergency department visits. Epidemiology. 16(2):164-74.

Roy, A. A., Wagstrom, K. M., Adams, P. J., Pandis, S. N., Robinson, A. L., 2011. Quantification of the effects of molecular marker oxidation on source apportionment estimates for motor vehicles, Atmospheric Environment, 45, 3132-3140.

Roy, A. A., Adams, P. J., Robinson, A. L., 2014. Air pollutant emissions from the development, production, and processing of Marcellus Shale nature gas. J. of the Air and Waste Manage. Assoc., 64:1, 19-37.

Shaheen, S. and Cohen, A., 2013. Innovative mobility carsharing outlook. Transportation Sustainability Research Center, University of California at Berkeley.

Sarnat, J. A., Sarnat, S. E., Flanders, W. D., Chang, H. H., Mulholland, J., Baxter, L., Isakov, V., Ozkaynak, H., 2013. Spatiotemporally resolved air exchange rate as a modifier of acute air pollution-related morbidity in Atlanta. J. Expo. Sci. Environ. Epidemiol. 23, 606-615.

Schildcrout, J. S., Sheppard, L., Lumley, T., Slaughter, J. C., Koenig, J. Q., Shapiro, G. G., 2006. Ambient air pollution and asthma exacerbations in children: an eight-city analysis. Am. J. Epidemiol., 164(6), 505-517.

Shimadera, H., Hayami, H., Chatani, S., Morino, Y., Mori, Y., Morikawa, T., Yamaji, K., Ohara, T., 2014. Sensitivity analyses of factors influencing CMAQ performance for fine particulate nitrate. J. Air and Waste Manage. Assoc., 64:4, 374-387.

Skamarock, W. C., and Klemp, J. B., 2008. A time-split non-hydrostatic atmospheric model for weather research and forecasting applications. J. Comput. Phys., 227, 3465-3485.

Soret, A., Guevara, M., Baldasano, J.M., 2014. The potential impacts of electric vehicles on air quality in the urban areas of Barcelona and Madrid (Spain). Atmos. Environ., 99, 51-63.

TCEQ, 2015. On Road, Mobile Source Trend Emissions Inventories for All 254 Counties in Texas for 1999 – 2050. Prepared by the Texas Transportation Institute, August 2015. https://www.tceq.texas.gov/assets/public/implementation/air/am/contracts/reports/mob/5821111226FY1514-20150807-tti-MOVES2014_Onroad_EI_Trends_1990_2050.pdf

TCEQ, 2001. Texas Emissions Reduction Plan (TERP). https://www.tceq.texas.gov/airquality/terp/.

Tessum, C. W., Hill, J. D., Marshall, J. D., 2014. Life cycle air quality impacts of conventional and alternative light-duty transportation in the United States. Proceedings of the National Academy of Sciences, 111, 52, 18490-18495.

Thompson, T., Webber, M., Allen, D. T., 2009. Air quality impacts of using overnight electricity generation to charge plug-in hybrid electric vehicles for daytime use. Environ. Res. Lett., 4, 014002.

Thompson, T. M., King, C. W., Allen, D. T., Webber, M. E., 2011. Air quality impacts of plug-in hybrid electric vehicles in Texas: evaluating three battery charging scenarios. Envrion. Res. Lett., 6, 024004.

U.S. DOE, 2018. Energy Information Administration (EIA)'s Annual Energy Outlook of 2018 (AEO2018). https://www.eia.gov/outlooks/aeo/pdf/AEO2018.pdf.

U.S. EPA, 2015a. Technical support document: preparation of emissions inventories for the version 6.2, 2011 emissions modeling platform, August, 2015.

U.S. EPA, 2015b. 2011 National Emissions Inventory, version 2, technical support document, August, 2015.

U.S. EPA, 2015c. Population and Activity of On-road Vehicles in MOVES2014, Draft Report. EPA-420-D-15-001, July, 2015.

U.S. EPA, 2016. MOVES2014a: Latest Version of MOtor Vehicle Emission Simulator (MOVES). https://www.epa.gov/moves/moves2014a-latest-version-motor-vehicle-emission-simulator-moves

U.S. EPA, 2017a. SPECIATE Data Browser. https://cfpub.epa.gov/speciate/

U.S. EPA, 2017b. Environmental Benefits Mapping and Analysis Program: Community Edition (BenMAP-CE) User Manual and Appendices. Research Triangle Park, NC, USA. April, 2017.

U.S. EPA, 2017c. Emissions and Generation Resource Integrated Database (eGRID), eGRID2014, version 2, Feb 27, 2017. https://www.epa.gov/energy/emissions-generation-resource-integrated-database-egrid

U.S. EPA Green Book, 2017. 8-Hr Ozone (2008) Nonattainment State/Area/County Report, as of September 30, 2017. http://www.epa.gov/airquality/greenbook/hncs.html#TEXAS.

Vaughan, A, 2017. Norway leads way on electric cars: 'it's part of a green taxation shift'. The Guardian, Dec 25, 2017. https://www.theguardian.com/environment/2017/dec/25/norway-leads-way-electric-cars-green-taxation-shift.

Walsh, M. P., 2017. Carlines. http://walshcarlines.com/index.html.

Wilson A. M., Wake, C. P., Kelly, T., et al, 2005. Air pollution and weather, and respiratory emergency room visits in two northern New England cities: an ecological time-series study. Environ. Res., 97(3): 312-21.

Woods & Poole Economics Inc., 2015. Complete Demographic Database. Washington, DC. https://www.woodsandpoole.com/

Yarwood, G., Rao, S., Yocke, M., Whitten, G.Z., 2005. Updates to the Carbon Bond chemical mechanism: CB05. Final Report to the US EPA, RT-0400675, December 8, 2005. http://www.camx.com/publ/pdfs/CB05_Final_Report_120805.pdf.

Zanobetti, A., and Schwartz, J., 2008. Mortality displacement in the association of ozone with mortality: an analysis of 48 cities in the United States. Am J Respir Crit Care Med, 177, 184-189.

Zhang, R., Wang, G., Guo, S., Zamora, M. L., Ying, Q., Lin, Y., Wang, W., Hu, M., Wang, Y., 2015. Formation of urban fine particulate matter, Chem. Rev., 115, 3803-3855.